JCTC Journal of Chemical Theory and Computation

Article

pubs.acs.org/JCTC

The Variationally Orbital-Adapted Configuration Interaction Singles (VOA-CIS) Approach to Electronically Excited States

Xinle Liu and Joseph E. Subotnik*

Department of Chemistry, University of Pennsylvania, Philadelphia, Pennsylvania 19104, United States

ABSTRACT: For chemically accurate excited state energies, one is forced to include electron−electron correlation at a level of theory significantly higher than configuration interaction singles (CIS). Post-CIS corrections do exist, but most often, if they are computationally inexpensive, these methods rely on perturbation theory. At the same time, inexpensive *variational* post-CIS methods would be ideal since modeling electronic relaxation usually requires globally smooth potential energy surfaces (PESs) and there will inevitably be regions of near electronic degeneracy. With that goal in mind, we now present a new method entitled variationally orbital adapted CIS (VOA-CIS). On the one hand, we show that in the ground-state geometry, VOA-CIS performs comparably to CIS(D) at predicting relative excited state energies. On the other hand, far beyond CIS(D) or any other perturbative method, VOA-CIS correctly rebalances the energy of charge-transfer (CT) states versus non-CT states, while simultaneously producing smooth PESs—including the important case of avoided crossings. In fact, through localized diabatization of VOA-CIS excited states, one can find a set of reasonable diabatic states modeling CT chemical dynamics. After significant benchmarking, we are now confident VOA-CIS and VOA-CIS-like methods should play a major role in future excited state calculations.

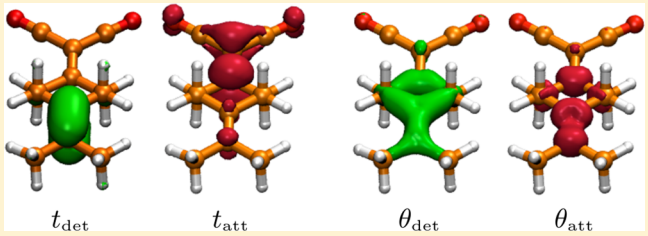

I. INTRODUCTION

Our research group desperately needs practical, inexpensive methods for modeling excited states: such methods must be (i) inexpensive and applicable to large molecules and (ii) accurate enough to capture excited state crossings (which are essential for understanding electronic relaxation).

Configuration interaction singles (CIS) is perhaps the simplest approach to electronic excited states. One assumes that an excited state wave function is a linear combination of single excitations on top of the ground state. On the plus side, CIS is variational, size-consistent, and most of the time, CIS-wave functions are qualitatively correct (in terms of detachment and attachment plots[1]). On the negative side, CIS energies are simply not accurate and one cannot ascertain relative excited state energies from a CIS calculation alone: the CIS ansatz captures too little electron correlation and thus represents too great a simplification of the excited state wave functions for chemical accuracy. One cardinal failure of CIS is its notorious overestimation of charge-transfer (CT) excited state energies by 1−2 eV.[2]

The goal of this paper is to introduce a new and powerful method that builds a variational wave function on top of zeroth-order CIS wave function.[3] The format of this paper will be as follows. In section II, we review existing post-CIS excited state methods and motivate our new VOA-CIS approach. In section III, we provide the theoretical framework for VOA-CIS as well as the computational details for extracting VOA-CIS wave functions and energies. In section IV, we benchmark VOA-CIS excited states versus results from high-level approaches in excited state theory and experimental data. In section V we present a brief and pictorial discussion of how and why VOA-CIS works and its close connection with time-dependent HF (TDHF).[4,5] We conclude in section VI with a summary of the VOA-CIS approach and a look toward future extensions, theoretical and computational.

Notation. Throughout this paper, *ijkl*, *abcd*, and *pqrs* denote occupied, virtual, and any molecular orbitals (MOs), respectively. *IJKL* are the indexes for CIS states and *G* is always the ground state, while $\tilde{I}\tilde{J}\tilde{K}\tilde{L}$ will signify either the ground or an excited state. Lowercase *o* will signify an occupied entry, while lowercase *v* will signify a virtual entry.

II. BACKGROUND: POST-CIS METHODS

A. CIS(D). The simplest post-CIS excited state methodology is CIS(D). CIS(D)[6] proposes a perturbative improvement to CIS, modeled roughly after CIS-MP2.[7] Whereas CIS-MP2 applies standard perturbation theory in the entire doubles and triples space $\{|\Phi_{ij}^{ab}\rangle, |\Phi_{ijk}^{abc}\rangle\}$, CIS(D) applies standard perturbation theory only in the doubles space; for the triples space, CIS(D) hypothesizes a first-order wave function correction via an intuitive ansatz, rather than strictly applying formal perturbation theory: CIS(D) proposes that the amplitudes for triply excited excitations are the products of CIS singles excitations with ground-state MP2 double excitations. The validity of this hypothesis can be tested numerically. In the end, the CIS(D) correction can be broken up into three parts: one component from the doubles manifold, and two components from the triples manifold—one

Received: October 25, 2013
Published: February 4, 2014

 © 2014 American Chemical Society dx.doi.org/10.1021/ct4009377 | J. Chem. Theory Comput. 2014, 10, 1004−1020

"disconnected" and one "connected" component. The disconnected component cancels exactly with the ground-state MP2 energy, and the resulting two terms make up the vertical excitation energy. The final CIS(D) energy is size-consistent (unlike CIS-MP2) and the overall cost of the method is $O(N^5)$.

Although CIS(D) reduces the computational cost of CIS-MP2 from $O(N^6)$ to $O(N^5)$, as N gets big, the amount of work increases quickly. Luckily, in recent years, through the implementation of the resolution-of-the-identity (RI) approximation,[8,9] the CIS(D) prefactor has been reduced greatly, and currently the method is applicable to the calculation of vertical excitation energies in small to medium-sized molecules; local pair-natural orbital approaches can further reduce the cost.[10] That being said, CIS(D) still cannot be implemented to help solve most problems in electronic relaxation. Beyond the failure of CIS(D) to capture enough electron−electron correlation energy for CT states,[2] the biggest culprit is the perturbative nature of the CIS(D) ansatz itself. In general, electronic relaxation (as mediated by phonons or nuclear motion) occurs at nuclear geometries where several electronic states come close together in energy; this is the entire basis of classical Marcus theory.[11,12] At such geometries, however, the use of perturbation theory is usually not valid: the zeroth order wave functions can still be strongly interacting and, in such cases, the resulting CIS(D) wave functions and energy corrections will be unreliable. Thus, in the end, CIS(D) can be used to model only those electronic states that are well-separated energetically; the method also fails if the S_0−S_1 gap becomes too small and there is strong mixing between ground and excited states. Note that these limitations apply to all perturbative excited state methods.

B. CIS(D_n) and CC2. As a nondegenerate perturbative method, CIS(D) cannot deal with near-degeneracies. Among the set of post-CIS excited state methods, CIS(D_n)[13] is a quasi-degenerate improvement to CIS(D). CIS(D_n) was designed around the principle of "perturb and then diagonalize". The CIS(D_n) correction is found by diagonalizing a perturbative approximation to the second-order response matrix for the MP2 ground state.

Within the CIS(D_n) framework, one always approximates the doubles−doubles block of the response matrix by excitations of the diagonal Fock matrix. If this is the only enforced approximation, diagonalization of the response matrix is entitled CIS(D_∞), which closely resembles[14] the CC2[15] method. Otherwise, one can expand the self-energy of the doubles−doubles block in a Taylor series, and with truncation one generates CIS(D_0) and CIS(D_1) . Formally, CIS(D_0) and CIS(D_1) require diagonalization of a dressed matrix with size $N_{ov} \times N_{ov}$, just like CIS; CIS(D_∞) requires diagonalization of a matrix of size $N_{ov}^2 \times N_{ov}^2$ (through several tricks help). In practice, full CIS(D_0) and CIS(D_1) are significantly more expensive than CIS(D) calculations.

Overall, the CIS(D_n) suite of algorithms are a powerful means to investigate avoided crossings between excited states, but they suffer from several drawbacks:

- The computational cost can be prohibitive. Recently, progress has been made to reduce the cost of CIS(D_0) through an empirically scaled opposite-spin (SOS) approximation.[16] For CC2 methods, local approximations with density fitting have also been made,[17] as have pair natural orbital approaches.[18]
- For $n > 0$, the CIS(D_n) effective Hamiltonian is not Hermitian, and thus, the method can fail at near-degeneracies, especially near conical intersections where imaginary frequencies are possible.[14] To improve upon CC2 near a true degeneracy, the algebraic diagrammatic construction (ADC) method[19] symmetrizes the response matrix and thus one must diagonalize only a Hermitian matrix.
- The CIS(D_n) approach will not be effective when the S_0−S_1 energy gap becomes too small, or when doubly excited states are important.

C. ADC(2). A natural alternative to CIS(D_∞) (or CC2) with the flavor of configuration interaction is the algebraic diagrammatic construction (ADC) method.[19] (For a complete set of ADC(2) references, see ref 20.) As mentioned above, the ADC(2) method symmetrizes the CC2 response matrix and thus one must diagonalize only a Hermitian matrix; thus, the method is applicable near avoided crossings as well as conical intersections. Importantly, ADC(2) yields a means to calculate electronic matrix elements between excited states[21] which is useful for electronic dynamics.[22] Unfortunately, the cost of the method is approximately the cost of a CC2 calculation, which can be prohibitive for large systems, even though local approximations are possible.[18] S_0−S_1 crossings will also be difficult to converge (as with any single reference ground-state theory).

Lastly, it must be noted that one can go beyond strict ADC(2) via the ADC(2)-x algorithm[23] that includes all off-diagonal terms in the doubles−doubles block of the effective Hamiltonian. Thus, ADC(2)−x allows for the possibility of doubly excited states, but the cost of ADC(2)−x grows accordingly (as N^6, on the order of EOM-CCSD). Overall, ADC is a promising approach for generating the excited states necessary for describing electronic relaxation, but computational cost remains an obstacle (and S_0−S_1 crossings are a potential problem).

D. CISD. According to the standard quantum chemistry dogma, the formal answer to all problems in electronic structure theory is full-CI. However, full-CI requires diagonalization of the Hamiltonian at all levels of excitation. As such, full-CI has an exponentially large cost and is practical only for very small molecules. For medium-sized or large molecules, if one is keen on configuration interaction, one must settle for truncated-CI—which is still variational but unfortunately not size-consistent. The accuracy of truncated CI deteriorates as the number of electrons increases, though corrections for recovering size-consistency are well-known for CISD.[24]

Now, it is important to recognize that CISD's size-consistency problem for excited states can be partially removed by excluding the HF ground-state from the Hamiltonian diagonalization. In such a case, intuitively, if we have two infinitely separated fragments A and B, excitations localized to fragment A (set no. 1) are entirely decoupled from excitations localized to fragment B (set no. 2). The only problematic complication is that we can find a third set (set no. 3) of excited states with excitations on both fragments A and B. However, this third set of excitations is entirely decoupled from set nos. 1 and 2, and thus, by inspection, one can pick out excited states with size-consistent wave functions and energies. For more details, see the Appendix.

Despite this glimmer of hope, however, we must emphasize that straight CISD necessarily produces poor excitation

energies. On the one hand, if the HF state is excluded, excitation energies are always too low—after all, only the excited states are stabilized with correlation energy. On the other hand, if we include the HF state, CISD is known to overstabilize the ground state[25] and yield erroneously large excitation energies (see also Figure 1 below). This failure of

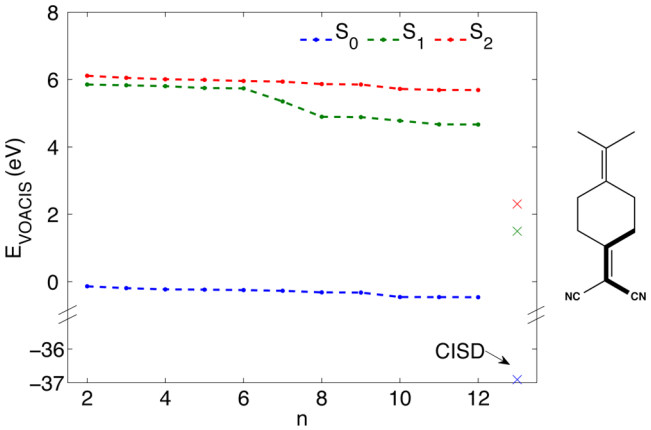

Figure 1. Comparison of VOA-CIS-G(n, 2) energies with (approximate) CISD energies[30] at the ground state geometry, for the first three singlet states. The zero of energy for this figure is E_{HF}. On the right is the PYCM molecular structure, with the dihedral angle τ shown with bold bonds. Note that VOA-CIS excitation energies are close to experimental values and relatively insensitive to n for n not too big and not too small ($n \in [8, 12]$). Here, S_1 is the CT state and finds a big correction with $n = 8$ (because CIS orders this state as S_7). By contrast, note that CISD excitation energy are grossly unphysical (with $E_1 - E_0 = 38.41$ eV!).

CISD results from the fact that the ground and excited states are not treated equivalently: while the ground state couples strongly to the doubles space and gains a great deal of dynamical correlation, a CIS excited state wave function will not relax sufficiently without inclusion of the corresponding triples space. In the end, the variational benefits of full CISD must be weighed against the distorted CISD absolute vertical excitation energies. (For a discussion of multireference configuration interaction in the context of the VOA-CIS algorithm below, please see the Appendix.)

E. Perturbative Orbital Optimized CIS (OO-CIS). Using all of the background above, over the past few years our research group has been working to develop our own post-CIS excited state methods. Given that CIS states are strongly coupled to the space of double excitations (on the one hand) but including entire doubles space *a la* CISD is counterproductive (on the other hand), our original intuition was that meaningful post-CIS excited state wave functions could be obtained by partial orbital optimization. In particular, our hope was that reasonably accurate excited state energies could be obtained by optimizing the MOs for each specific excited state, rather than always using the same SCF orbitals that were optimized for the ground state. Moreover, as long as the orbital changes were small, each excited state would keep its identity and the algorithm would remain stable. The end product of this line of thinking was an algorithm entitled perturbatively orbital optimized CIS (OO-CIS).[26]

According to the OO-CIS algorithm, we start from CIS wave functions which diagonalize the Hamiltonian in the singles space:

$$\mathbf{A} \equiv \langle \Phi_i^a | H | \Phi_j^b \rangle, \qquad \sum_{bj} A_{aibj} t_j^{bI} = E_{\mathrm{CIS}}^I t_i^{aI}$$

with corresponding energies:

$$E_{\mathrm{CIS}}^I = E_{\mathrm{HF}} + \sum_{abi} t_i^{aI} t_i^{bI} F_{ab} - \sum_{aij} t_i^{aI} t_j^{aI} F_{ij} + \sum_{abij} t_i^{aI} t_j^{bI} \langle aj \| ib \rangle$$

It is not difficult to prove that, because of their variational nature, the CIS amplitudes ($\{t^I\}$) are fully optimized fore each excited state. At the same time, though, the MOs for CIS states are calculated via a HF calculation and thus optimized with respect to the ground state; as such, the MOs are certainly not optimized for excited states.

To achieve partial orbital optimization, note that any MO $\{|\phi_p\rangle\}$ is defined in terms of atomic orbitals (AOs) by its matrix of MO coefficients $\mathbf{C}$:

$$|\phi_p\rangle = \sum_{\mu} |\chi_\mu\rangle \mathbf{C}_{\mu p}$$

At this point, we can perform a unitary transformation of the MOs by introducing an antisymmetric matrix Θ

$$\Theta = \sum_{p>q} \theta_{pq} \mathbf{J}_{pq}, \qquad (\mathbf{J}_{pq})_{rs} \equiv -\delta_{pr}\delta_{qs} + \delta_{ps}\delta_{qr}$$

and exponentiating[27]

$$C_{\mu p} = \sum_q C_{\mu q}{}^0 U_{qp} \equiv \sum_q C_{\mu q}{}^0 (e^{\Theta})_{qp}$$

Now the MOs are parametrized uniquely and nonredundantly by Θ.[27] Fortunately, $\theta_{ij}^{\mathrm{opt}}$ and $\theta_{ab}^{\mathrm{opt}}$ turn out to be zero, and only $\theta_{ai}^{\mathrm{opt}}$ survives. Assuming all components of Θ are small, one can expand the energy expression up to second-order:

$$E_{\mathrm{CIS}}(\Theta) = E_{\mathrm{CIS}}(0) + \sum_{ai} Y_{ai}\theta_{ai} + \frac{1}{2}\sum_{aibj} \left.\frac{\partial^2 E_{\mathrm{CIS}}}{\partial\theta_{ai}\partial\theta_{bj}}\right|_{\Theta=0} \theta_{ai}\theta_{bj} \tag{1}$$

and then minimize the CIS energy by taking a Newton–Raphson step from the original MOs C^0 ($\Theta^0 = 0$). The resulting θ and energy expressions are

$$\theta_{ai}^{\mathrm{opt}} = -\sum_{bj} \left(\left.\frac{\partial^2 E_{\mathrm{CIS}}}{\partial\theta_{ai}\partial\theta_{bj}}\right|_{\Theta=0} \right)^{-1} Y_{bj} \tag{2}$$

$$E_{\mathrm{CIS}}^{\mathrm{opt}} = E_{\mathrm{CIS}}(0) - \frac{1}{2}\sum_{aibj} Y_{ai} \left(\left.\frac{\partial^2 E_{\mathrm{CIS}}}{\partial\theta_{ai}\partial\theta_{bj}}\right|_{\Theta=0} \right)^{-1} Y_{bj} \tag{3}$$

Lastly, one final approximation is possible: we can approximate $\partial^2 E_{\mathrm{CIS}}/\partial\theta_{ai}\partial\theta_{bj}$ by the diagonal Fock matrix elements

$$\frac{\partial^2 E_{\mathrm{CIS}}}{\partial\theta_{ai}\partial\theta_{bj}} = \delta_{ij}\delta_{ab}(\varepsilon_a - \varepsilon_i) \tag{4}$$

so that the inversion in eqs 2 and 3 is trivial. In that case, let us define the following quantities:

$$-\frac{1}{2}Y_{ai}^{IJ} \equiv +\sum_{bcjk} t_k^{cI}\langle\Phi_k^c|\hat{H}a_a^\dagger a_i|\Phi_j^b\rangle t_j^{bJ}$$
$$= +\sum_{bcj}\left(t_i^{cI}t_j^{bJ}\langle cj||ab\rangle + t_j^{cI}t_j^{bJ}\langle ci||ba\rangle\right)$$
$$+\sum_{bjk}\left(t_k^{aI}t_j^{bJ}\langle ij||bk\rangle + t_k^{bI}t_j^{bJ}\langle ij||ka\rangle\right) \quad (5)$$

$$\theta_{ai}^{IJ} \equiv -\frac{Y_{ai}^{IJ}}{\varepsilon_a - \varepsilon_i + E^J - E^I} \quad (6)$$

With these definitions, the Newton−Raphson step above (eq 2) for electronic state I will yield: $\theta_{ai}^{\mathrm{opt}} \equiv \theta_{ai}^{II}$. Henceforward, we can easily construct the OO-CIS wave function for each state to first order in θ:

$$|\Psi_{\text{OO-CIS}}\rangle \approx |\Psi_{\text{CIS}}\rangle + \sum_{ai} t_i^a\theta_{ai}^{\mathrm{opt}}|\Phi_{\text{HF}}\rangle + |\Psi_{\text{OO-CIS}}^{(1)}\rangle$$
$$|\Psi_{\text{OO-CIS}}^{(1)}\rangle = -\sum_{abij} t_i^{aI}\theta_{bj}^{II}|\Phi_{ij}^{ab}\rangle$$
$$= -\sum_{bj}\theta_{bj}^{II}a_b^\dagger a_j|\Psi_{\text{CIS}}^I\rangle \equiv |\Psi_{\text{OO-CIS}}^{III}\rangle \quad (7)$$

Equation 7 defines the OO-CIS algorithm.

In practice, OO-CIS has some appealing properties. First, although we invoke orbital optimization in spirit for each CIS state, all optimization is actually performed with the initial SCF orbitals; this approach is completely free from cherry picking orbitals in an active space. Second, the algorithm is incredibly fast and not demanding.

Despite these attributes, however, the OO-CIS method is still perturbative (like CIS(D)), and we have found empirically that it yields significant improvement only for charge-transfer states (and, even then, the CT correction is not large enough). Lastly, because the excited states are nonorthogonal to the ground state, transition moments might be difficult to extract. Ideally, one would like an excited state approach with the speed of OO-CIS, but the accuracy of a balanced variational calculation (which can treat S_I−S_J crossings for all I, J).

III. VARIATIONAL ORBITAL ADAPTED CIS (VOA-CIS)

With the previous background material in mind, we now describe the VOA-CIS approach. In the spirit of CIS(D_n) (and also CIS(2)[28]), our intention is to perturb-then-diagonalize, rather than vice versa; however, unlike the case of CIS(D_n), we will formally use the full Hamiltonian matrix rather than an approximate response matrix. Thus, the VOA-CIS approach can be decomposed into two primary steps. First, we will generate a basis of wave functions in the spirit of a *generalized* OO-CIS approach. On the one hand, it is computationally cheap to generate perturbative wave functions through orbital optimization; on the other hand, we believe that orbital optimization should capture the most important doubles correction for excited states. Second, we diagonalize the Hamiltonian in the basis of all perturbed wave functions, thus yielding variational energies and eigenvectors. All Hamiltonian matrix elements can be evaluated through second-quantization and, in simplified form, the matrix elements are given in eqs 17, 18, and 19.

We will now discuss these steps in more detail. In the end, the notation for our algorithm can be cast in the form VOA-CIS-$C(n, m)$; in what follows, we will explain the meaning of C, n, and m.

A. Choosing the VOA-CIS Basis. We will define N_B as the size of the VOA-CIS basis.

1. Size of CIS Subspace (n). In choosing a set of basis functions for diagonalization, the first and most immediate question is the number of requested excited states. Very often, photochemical experiments can be interpreted by considering the dynamics of the lowest 10 excited states. This fortunate circumstance forms the basis for the entire VOA-CIS algorithm. Effectively, the VOA-CIS approach uses CIS as a means of generating a set of many-electron excited states as an "active" space. We define n as the number of CIS states which must be calculated initially (i.e., $N_B = n$), and the smaller n is, the faster the VOA-CIS algorithm will be. Although our algorithm will not be independent of n, luckily, from our experience,[3] VOA-CIS excited state wave functions and absolute energies do not change greatly with n; n can be chosen robustly. At the same time, though, the VOA-CIS ground-state will change dramatically as n gets very large and the VOA-CIS energy approaches the CISD limit; see the energy diagram in Figure 1 . This difference in behavior as a function of n will actually be exploited later.

Additional parameters we use are m and C. Roughly speaking, m is an indication of how many doubles we have for perturbed wave functions, while C tells how the ground state should be balanced against the excited states . The details are shown below.

2. Size of Doubles Space (m). Having picked an initial size for the CIS subspace n ($N_B = n$), we must next address the number of double excitations to be included in the (post-CIS) VOA-CIS basis. As mentioned above, we will select candidate doubles excitations using a *generalized* OO-CIS framework, with the following mathematical structure: $\{|\Psi^{IJK}\rangle \equiv -\sum_{bj}\theta_{bj}^{IJ}a_b^\dagger a_j|\Psi_{\text{CIS}}^K\rangle\}$. See eq 6 for a definition of θ; recall that I is the index of the CIS state from which the doubles are generated. In general, there are three nested options for choosing the number of such double excitations:

1. $\{|\Psi^{III}\rangle\}$ ($m = 1$): For the $m = 1$ case, VOA-CIS adds n doubly excited wave functions to the basis, on top of the original n CIS wave functions ($N_B+ = n$). These n wave functions are exactly the same as the first order wave functions one constructs by allowing for orbital relaxation in perturbative OO-CIS . See equation eq 7 in section II.E above.
2. $\{|\Psi^{IJJ}\rangle\}$ ($m = 2$): For the $m = 2$ case, VOA-CIS adds n^2 doubly excited wave functions to the basis, on top of the original n CIS wave functions ($N_B+ = n^2$). These n^2 wave functions include all wave functions proposed in the $m = 1$ case. Now, the basic idea is to expand each of the n excited CIS states in a basis of doubly excited states that can be generated by single excitations from those same n excited states. This gives n^2 different combinations of the form $\{|\Psi^{IJJ}\rangle\}$. The $m = 2$ subspace is a clear improvement over the $m = 1$ subspace because, at an avoided crossing, excited states will begin to mix and thus, in order to capture electron−electron correlation correctly, we must allow for mixing between the doubly excited configurations generated from different CIS states.
3. $\{|\Psi^{IJK}\rangle\}$ ($m = 3$): For the $m = 3$ case, VOA-CIS adds n^3 doubly excited wave functions to the basis, on top of the original n CIS wave functions ($N_B+ = n^3$). These n^3 wave

Table I. Additional Basis Functions Included Alongside the CIS States $\{|\Psi^I_{\mathrm{CIS}}\rangle\}$ for VOA-CIS-C(n, m)[a]

	C							
m	O		G		X			
1	$\|\Psi^{JJJ}\rangle$	$(2n)$	$\|\Phi_{\mathrm{HF}}\rangle$,	$\|\Psi^{JJJ}\rangle$ $(1 + 2n)$	$\|\Phi_{HF}\rangle$,	$\|\Psi^{JJJ}\rangle$		$(1 + 2n)$
2	$\|\Psi^{JKK}\rangle$	$(n + n^2)$	$\|\Phi_{\mathrm{HF}}\rangle$,	$\|\Psi^{JKK}\rangle$ $(1 + n + n^2)$	$\|\Phi_{\mathrm{HF}}\rangle$,	$\|\Psi^{JKK}\rangle$,	$\|\Psi^{GKK}\rangle$	$(1 + 2n + n^2)$
3	$\|\Psi^{JKL}\rangle$	$(n + n^3)$	$\|\Phi_{\mathrm{HF}}\rangle$,	$\|\Psi^{JKL}\rangle$ $(1 + n + n^3)$	$\|\Phi_{\mathrm{HF}}\rangle$,	$\|\Psi^{JKL}\rangle$,	$\|\Psi^{GKL}\rangle$,	$(1 + n + n^2 + n^3)$

[a] I, J, K, L = {1, 2, ..., n}. In parentheses, we give the total number of basis wavefunctions (N_{B}) for each option.

functions include all wave functions proposed in the m = 2 case, but there is no physical basis for including all $\{|\Psi^{IJK}\rangle\}$ (m = 3) in the VOA-CIS basis. Instead, the only justification that can be given is mathematical: notice that the m = 3 basis is well-defined even at a point of exact degeneracy between two CIS states. The same conclusion is not true for the m = 1 or m = 2 subspaces.

3. Treatment of Ground State (C). The final question that must be addressed for the VOA-CIS basis is our treatment of the ground state. On the one hand, for an exactly size-consistent algorithm, one should exclude the ground state from the basis. (See the Appendix for a proof.) On the other hand, without including the ground state, a post-CIS algorithm cannot construct meaningful wave functions and energies whenever the ground state is energetically close to the first excited state (which is not uncommon far from the equilibrium geometry). Facing this dilemma, we believe that most often the correct choice is to include the ground-state, while also comparing results with the case of ground-state exclusion.

In the end, just as for the choice of double spaces, we can define three nested possible routes by which VOA-CIS can treat the ground state. These options are defined through the parameter C:

1. C = O: When considering the ground-state, the simplest option is to ignore the ground state and not include the Hartree−Fock determinant in the VOA-CIS basis. Thus, N_{B} is unchanged. We label this option "O". In this case, one recovers exact size-consistency.
2. C = G: Vice versa, the next simplest option is simply to include the HF determinant in the basis, which we label the "G" option (N_{B}+ = 1). The G option is especially important when the S_0−S_1 energy gap gets small and ground-excited state mixing is unavoidable. In such cases, it make sense to forego exact size-consistency for the sake of reasonable energetics around an avoided crossing. Moreover, ref 3 showed that, in the case of twisted ethylene, VOA-CIS excitation energies are not changed greatly by including the HF determinant. In fact, VOA-CIS-G excitation energies are well-balanced; unlike CISD, the VOA-CIS-G ground state is not overstabilized relative to the excited states and VOA-CIS yields reliable absolute excitation energies.
3. C = X: We label our third and final option for treating the ground state with the letter "X". For this option, we include not only the Hartree−Fock determinant in our basis, but we also include the doubly excited determinants generated by the interaction of the HF state with single excitations on top of CIS states.

   Mathematically, just as one CIS state can be expanded in a basis of orbital optimized CIS states, so too can the HF ground state be expanded in a basis of orbital optimized CIS states. Thus, just as was done previously, one can define a set of doubly excited determinants $\{|\Psi^{GJK}\rangle\}$ to relax the HF ground state. These doubly excited determinants are defined analogously to eqs 5 and 6 through the intermediate quantities Y^{GJ} and θ^{GJ}:

$$-\frac{1}{2}Y^{\mathrm{GJ}}_{ai} \equiv \langle \Phi_{\mathrm{HF}}|Ha^{\dagger}_a a_i|\Psi^J_{\mathrm{CIS}}\rangle = \sum_{bj} t^{bJ}_j \langle ij||ab\rangle \tag{8}$$

$$\theta^{\mathrm{GJ}}_{ai} = -\frac{Y^{\mathrm{GJ}}_{ai}}{\varepsilon_a - \varepsilon_i + E^J_{\mathrm{CIS}} - E_{\mathrm{HF}}} \tag{9}$$

In section V.B, we will show that this "X" option is closely related to the TDHF formalism.

- For the case of m = 1, the "X" option is redundant; the electronic bases in VOA-CIS-G(n, 1) and VOA-CIS-X(n, 1) are exactly the same (N_{B}+ = 1).
- For the case m = 2, we include all $\{|\Psi^{GJJ}\rangle\}$, and so we set N_{B} + = n.
- For the case m = 3, we include all $\{|\Psi^{GJK}\rangle\}$, and so we set N_{B}+ = n^2.

4. Synopsis. In the end, there are as many as 9 (or really 8) different flavors of VOA-CIS . Henceforward, we will use the notation VOA-CIS-C(n, m), as defined in Table I . A priori, it would appear difficult to predict the optimal algorithm. Luckily, according to our experience, for large enough n, the relative energies among excited states remain almost unchanged for all choices. That being said, though, choosing the absolutely best *ground-state* option can be tricky and absolute excitation energies can change with choice of method. Thus far, if we seek the best absolute potential energy surfaces—including geometries far from equilibrium—VOA-CIS-G(n, 2) seems to be the best choice.

B. Matrix Elements for VOA-CIS. Having constructed a well-defined basis for excited state wave functions, we must now diagonalize the Hamiltonian. The necessary matrix elements for the Hamiltonian (H), overlap (S) and dipole ($\vec{\mathbf{R}} \equiv (X, Y, Z)$) operators are quite similar. Of course, the matrix elements for S and $\vec{\mathbf{R}}$ are simpler than those for H in that the former are purely single-electron operators. All necessary matrix elements are given in eqs 17, 18, and 19 . For convenience, we use several convenient intermediate quantities defined below: in eqs 10−16, M can be of any size while A, B, C, and D are all of size $N_v \times N_o$:

$$\mathcal{L}^{vo}_{pq}(A) \equiv \sum_{ai} \langle pi||qa\rangle A_{ai} \tag{10}$$

$$\mathcal{L}^{vv}_{pq}(M) \equiv \sum_{ab} \langle pb||qa\rangle M_{ab} \tag{11}$$

$$\mathcal{L}^{oo}_{pq}(M) \equiv \sum_{ij} \langle pj||qi\rangle M_{ij} \tag{12}$$

$$\mathcal{F}_{ai}(A) \equiv \mathcal{L}^{vo}_{ai}(A) + \sum_b F_{ab}A_{bi} - \sum_j A_{aj}F_{ji} \tag{13}$$

dx.doi.org/10.1021/ct4009377 | J. Chem. Theory Comput. 2014, 10, 1004−1020

$$\mathcal{K}_{ab}(A, B) = \mathcal{L}_{ab}^{vv}(AB^{\mathrm{T}}) - \mathcal{L}_{ab}^{oo}(B^{\mathrm{T}}A) \tag{14}$$

$$\mathcal{K}_{ij}(A, B) = \mathcal{L}_{ij}^{vv}(AB^{\mathrm{T}}) - \mathcal{L}_{ij}^{oo}(B^{\mathrm{T}}A) \tag{15}$$

$$\mathcal{M}(A, B, C, D) \equiv D\cdot(AB^{\mathrm{T}}C + CB^{\mathrm{T}}A) \tag{16}$$

$$\begin{aligned}
\langle\Phi_{\mathrm{HF}}|H|\Phi_{\mathrm{HF}}\rangle &= E_{\mathrm{HF}}\\
\langle\Psi_{\mathrm{CIS}}^{I}|H|\Psi_{\mathrm{CIS}}^{J}\rangle &= \delta_{IJ}E_{\mathrm{CIS}}^{J}\\
\langle\Psi^{\tilde{I}JK}|H|\Psi^{\tilde{I}'J'K'}\rangle &= \sum_{abij}\theta_{bj}^{\tilde{I}J}\theta_{ai}^{\tilde{I}'J'}\langle\Psi^{K}|a_j^{\dagger}a_bHa_a^{\dagger}a_i|\Psi^{K'}\rangle\\
&= +(t^{K}\cdot t^{K'})(\theta^{\tilde{I}J}\cdot\theta^{\tilde{I}'J'})E_{\mathrm{HF}}\\
&\quad + (t^{K}\cdot\theta^{\tilde{I}'J'})(\theta^{\tilde{I}J}\cdot t^{K'})E_{\mathrm{HF}}\\
&\quad - \mathcal{M}(\theta^{\tilde{I}J}, \theta^{\tilde{I}'J'}, t^{K}, t^{K'})E_{\mathrm{HF}}\\
&\quad - \mathcal{M}(\theta^{\tilde{I}J}, \theta^{\tilde{I}'J'}, t^{K}, \mathcal{F}(t^{K'}))\\
&\quad - \mathcal{M}(\theta^{\tilde{I}J}, t^{K'}, t^{K}, \mathcal{F}(\theta^{\tilde{I}'J'}))\\
&\quad - \mathcal{M}(\theta^{\tilde{I}J}, \theta^{\tilde{I}'J'}, \mathcal{L}_{vo}^{vo}(t^{K}), t^{K'})\\
&\quad - \mathcal{M}(t^{K}, t^{K'}, \mathcal{L}_{vo}^{vo}(\theta^{\tilde{I}J}), \theta^{\tilde{I}'J'})\\
&\quad + \theta^{\tilde{I}J}\cdot(\mathcal{K}_{vv}(t^{K'}, t^{K})\theta^{\tilde{I}'J'})\\
&\quad - \theta^{\tilde{I}J}\cdot(\theta^{\tilde{I}'J'}\mathcal{K}_{oo}(t^{K'}, t^{K}))\\
&\quad + \theta^{\tilde{I}J}\cdot(\mathcal{K}_{vv}(\theta^{\tilde{I}'J'}, t^{K})t^{K'})\\
&\quad - \theta^{\tilde{I}J}\cdot(t^{K'}\mathcal{K}_{oo}(\theta^{\tilde{I}'J'}, t^{K}))\\
\langle\Phi_{\mathrm{HF}}|H|\Psi_{\mathrm{CIS}}^{L}\rangle &= 0\\
\langle\Phi_{\mathrm{HF}}|H|\Psi^{\tilde{I}JK}\rangle &= \sum_{ai}\theta_{ai}^{\tilde{I}J}\langle\Phi_{\mathrm{HF}}|Ha_a^{\dagger}a_i|\Psi^{K}\rangle\\
&= \sum_{abij}\theta_{ai}^{\tilde{I}J}t_j^{bK}\langle ij\|ab\rangle\\
&= \theta^{\tilde{I}J}\cdot(\mathcal{L}_{ov}^{vo}(t^{K}))^{\mathrm{T}}\\
\langle\Psi_{\mathrm{CIS}}^{L}|H|\Psi^{\tilde{I}JK}\rangle &= \theta^{\tilde{I}J}\cdot(-2Y^{LK})
\end{aligned} \tag{17}$$

$$\begin{aligned}
\langle\Phi_{\mathrm{HF}}|X|\Phi_{\mathrm{HF}}\rangle &= X_{\mathrm{HF}}\\
\langle\Psi_{\mathrm{CIS}}^{I}|X|\Psi_{\mathrm{CIS}}^{J}\rangle &= \delta_{IJ}X_{\mathrm{HF}}^{I} + t^{I}\cdot(X_{vv}t^{J} - t^{J}X_{oo})\\
\langle\Psi^{\tilde{I}JK}|X|\Psi^{\tilde{I}'J'K'}\rangle &= \sum_{abij}\theta_{bj}^{\tilde{I}J}\theta_{ai}^{\tilde{I}'J'}\langle\Psi^{K}|a_j^{\dagger}a_bXa_a^{\dagger}a_i|\Psi^{K'}\rangle\\
&= +(t^{K}\cdot t^{K'})(\theta^{\tilde{I}J}\cdot\theta^{\tilde{I}'J'})X_{\mathrm{HF}}\\
&\quad + (t^{K}\cdot\theta^{\tilde{I}'J'})(\theta^{\tilde{I}J}\cdot t^{K'})X_{\mathrm{HF}}\\
&\quad - \mathcal{M}(\theta^{\tilde{I}J}, \theta^{\tilde{I}'J'}, t^{K}, t^{K'})X_{\mathrm{HF}}\\
&\quad - \mathcal{M}(\theta^{\tilde{I}J}, \theta^{\tilde{I}'J'}, t^{K}, (X_{vv}t^{K'} - t^{K'}X_{oo}))\\
&\quad - \mathcal{M}(\theta^{\tilde{I}J}, t^{K'}, t^{K}, (X_{vv}\theta^{\tilde{I}'J'} - \theta^{\tilde{I}'J'}X_{oo}))\\
&\quad + (t^{K}\cdot(X_{vv}t^{K'} - t^{K'}X_{oo}))(\theta^{\tilde{I}J}\cdot\theta^{\tilde{I}'J'})\\
&\quad + (t^{K}\cdot t^{K'})(\theta^{\tilde{I}J}\cdot(X_{vv}\theta^{\tilde{I}'J'} - \theta^{\tilde{I}'J'}X_{oo}))\\
&\quad + (t^{K}\cdot\theta^{\tilde{I}'J'})(t^{K}\cdot(X_{vv}\theta^{\tilde{I}'J'} - \theta^{\tilde{I}'J'}X_{oo}))\\
&\quad + ((X_{vv}t^{K} - t^{K}X_{oo})\cdot\theta^{\tilde{I}'J'})(t^{K'}\cdot\theta^{\tilde{I}J})\\
\langle\Phi_{\mathrm{HF}}|X|\Psi_{\mathrm{CIS}}^{L}\rangle &= t^{L}\cdot X_{vo}\\
\langle\Phi_{\mathrm{HF}}|X|\Psi^{\tilde{I}JK}\rangle &= 0\\
\langle\Psi_{\mathrm{CIS}}^{L}|X|\Psi^{\tilde{I}JK}\rangle &= + (t^{L}\cdot\theta^{\tilde{I}J})(t^{K}\cdot X_{vo})\\
&\quad + (t^{L}\cdot t^{K})(\theta^{\tilde{I}J}\cdot X_{vo})\\
&\quad - \mathcal{M}(t^{L}, t^{K}, X_{vo}, \theta^{\tilde{I}J})
\end{aligned} \tag{18}$$

$$\begin{aligned}
\langle\Phi_{\mathrm{HF}}|S|\Phi_{\mathrm{HF}}\rangle &= 1\\
\langle\Psi_{\mathrm{CIS}}^{I}|S|\Psi_{\mathrm{CIS}}^{J}\rangle &= \delta_{IJ}\\
\langle\Psi^{\tilde{I}JK}|S|\Psi^{\tilde{I}'J'K'}\rangle &= \sum_{abij}\theta_{bj}^{\tilde{I}J}\theta_{ai}^{\tilde{I}'J'}\langle\Psi^{K}|a_j^{\dagger}a_bSa_a^{\dagger}a_i|\Psi^{K'}\rangle\\
&= +(t^{K}\cdot t^{K'})(\theta^{\tilde{I}J}\cdot\theta^{\tilde{I}'J'})\\
&\quad + (t^{K}\cdot\theta^{\tilde{I}'J'})(\theta^{\tilde{I}J}\cdot t^{K'})\\
&\quad - \mathcal{M}(\theta^{\tilde{I}J}, \theta^{\tilde{I}'J'}, t^{K}, t^{K'})\\
\langle\Phi_{\mathrm{HF}}|S|\Psi_{\mathrm{CIS}}^{L}\rangle &= 0\\
\langle\Phi_{\mathrm{HF}}|S|\Psi^{\tilde{I}JK}\rangle &= 0\\
\langle\Psi_{\mathrm{CIS}}^{L}|S|\Psi^{\tilde{I}JK}\rangle &= 0
\end{aligned} \tag{19}$$

In algorithm 1, we provide a flowchart for how we have calculated VOA-CIS to date. Though this algorithm is not yet optimal or parallelized, it offers the reader a taste of how easy VOA-CIS energies and wave functions are to compute. In this flowchart, we define N_θ to be the number of $\theta^{\tilde{I}J}$s.

IV. RESULTS

The VOA-CIS algorithm was implemented in a developmental version of the Q-Chem[29] software package. We will now describe the results of applying the VOA-CIS algorithm to a broad range of photoexcitable organic molecules.

A. PYCM. *1. Absorption.* Over the last year, our research group has focused a great deal of attention on the molecule in Figure 1 (abbreviated PYCM for 2-(4-(propan-2-ylidene)-cyclohexylidene)malononitril).[31] Experimentally, PYCM has a low-lying CT absorption peak at 36 800 cm^{-1} (4.56 eV), where the donor (D) is the methylene group and the acceptor (A) is the dicyano group. Above the CT state, there is also a local A → A* excitation absorption peak on the cyano groups at 43 900 cm^{-1} (5.44 eV) (both in *n*-hexane at 20 °C).[32]

In Figure 1, we plot the dependence of the VOA-CIS energies (VOA-CIS-G(n, 2)) on the number of states n. All calculations were performed at the ground state geometry with the 6-31G* basis set (optimized with MP2), and we plot energies for the ground state and the first two excited states. S_1 is the CT state and S_2 is the locally excited state. On the right-hand side of Figure 1, we identify (approximate) CISD energies.[30] Recall that CISD energies are equivalent to VOA-CIS energies for $n = \infty$. Similar to our previous results for ethylene in ref 3, in Figure 1 we find again that CISD vastly overstabilizes the ground state; the vertical excitation energy of S_1 is a whoppingly unphysical 38.41 eV according to CISD.

By contrast, VOA-CIS-G(12, 2) yields far more balanced excitation energies than straight CISD, with S_1 having an excitation energy of 5.12 eV, which compares well with experiment (4.56 eV). Moreover, our results are not highly

dx.doi.org/10.1021/ct4009377 | J. Chem. Theory Comput. 2014, 10, 1004−1020

Algorithm 1: VOA-CIS algorithm

▷ Calculate $Y^{\tilde{I}J}$, $\theta^{\tilde{I}J}$
for I= $1:n$ **do** ▷ Calculate Y^{IJ}, θ^{IJ}
  for J= $1:n$ **do**
    $A = t^I; B = t^J$

$$-\frac{1}{2}Y_{ai}^{IJ} = +\sum_b \mathcal{L}_{ab}^{voT}(B)A_{bi} - \sum_j A_{aj}\mathcal{L}_{ji}^{voT}(B) + \mathcal{L}_{ai}^{vv}(AB^T) - \mathcal{L}_{ai}^{oo}(B^TA)$$

$$\theta_{ai}^{IJ} = -\frac{Y_{ai}^{IJ}}{E_{\mathrm{CIS}}^J - E_{\mathrm{CIS}}^I + \epsilon_a - \epsilon_i}$$

  end for
end for

for J= $1:n$ **do** ▷ Calculate Y^{GJ}, θ^{GJ}

$$-\frac{1}{2}Y_{ai}^{GJ} = \left(\mathcal{L}_{ia}^{vo}(t^J)\right)^T$$

$$\theta_{ai}^{GJ} = -\frac{Y_{ai}^{GJ}}{E_{\mathrm{CIS}}^J - E_{\mathrm{HF}} + \epsilon_a - \epsilon_i}$$

end for
$N_\theta = n^2 + n$
$N_B = n + 1 + n^2 + n^3$

for $\tilde{I}J$= $1:N_\theta$ **do** ▷ Normalize $\theta^{\tilde{I}J}$
  $\theta^{\tilde{I}J} = \theta^{\tilde{I}J}/\left|\theta^{\tilde{I}J}\right|$
end for

for I= $1:n$ **do** ▷ Save expensive matrices
  Save $\mathcal{L}_{ai}^{vo}(t^I)$, $\mathcal{F}_{ai}(t^I)$
end for
for $\tilde{I}J$= $1:N_\theta$ **do**
  Save $\mathcal{L}_{ai}^{vo}(\theta^{\tilde{I}J})$, $\mathcal{F}_{ai}(\theta^{\tilde{I}J})$
end for

for I= $1:n$ **do**
  for J= $1:n$ **do**
    A= $t^I; B = t^J$
    Save $\mathcal{K}_{ab}(t,t) = \mathcal{L}_{ab}^{vv}(AB^T) - \mathcal{L}_{ab}^{oo}(B^TA)$
    Save $\mathcal{K}_{ij}(t,t) = \mathcal{L}_{ij}^{vv}(AB^T) - \mathcal{L}_{ij}^{oo}(B^TA)$
  end for
end for
for $\tilde{I}J$= $1:N_\theta$ **do**
  for K= $1:n$ **do**
    A= $\theta^{\tilde{I}J}; B = t^K$
    Save $\mathcal{K}_{ab}(\theta,t) = \mathcal{L}_{ab}^{vv}(AB^T) - \mathcal{L}_{ab}^{oo}(B^TA)$
    Save $\mathcal{K}_{ij}(\theta,t) = \mathcal{L}_{ij}^{vv}(AB^T) - \mathcal{L}_{ij}^{oo}(B^TA)$
  end for
end for

▷ Construct the Hamiltonian
for $|\Psi_1\rangle \in \{ |\Phi_{\mathrm{HF}}\rangle, |\Psi_{\mathrm{CIS}}^L\rangle, |\Psi^{\tilde{I}JK}\rangle \}$ **do**
  for $|\Psi_2\rangle \in \{ |\Phi_{\mathrm{HF}}\rangle, |\Psi_{\mathrm{CIS}}^L\rangle, |\Psi^{\tilde{I}JK}\rangle \}$ **do**
    Save H_{12}, S_{12}, $\vec{\mathbf{R}}_{12}$
  end for
end for

for i= $1:N_B$ **do** ▷ Normalize Diagonals
  Factor= $\sqrt{S(i,i)}$
  for $M \in \{H, S, \vec{\mathbf{R}}\}$ **do**
    $M(i,:)/=$ Factor
    $M(:,i)/=$ Factor
  end for
end for

▷ $\{H, S, \vec{\mathbf{R}}, N_B\}$
$Hv = SvE \rightarrow \{v_i, E_i\}$, $i = 1, 2 \cdots N_B$
$\{v_i\} \rightarrow \{\vec{\mathbf{R}}_i$, Oscillator Strength $f_i\}$

dependent on n; the energy of the S_1 state changes sharply at n = 7 because the CT state is the seventh excited state according to CIS (but the CT state is the first excited state according to VOA-CIS). Finally, we mention that that VOA-CIS-G(12, 2) and VOA-CIS-O(12, 2) find very similar energies here for S_0, S_1, and S_2, relative to the original ground-state energy E_{HF} (not shown): −0.46, 4.66, and 5.69 eV versus 0.00, 4.66, and 5.66 eV. Altogether, on the basis of its reasonable excitation energies and its weak dependence on n, we find this data very encouraging and supportive of our claim that meaningful excited state energies can be found by diagonalizing only a sub-block of the CISD matrix.

2. Smooth PES and Emission. Regarding emission, experimentally the lower-lying PYCM CT state decays with measurable fluorescence, while the non-CT excited state decays exclusively radiationlessly. Verhoeven et al.[32] have postulated that these experimental signatures can be explained by breaking the ethylenic double bond connecting cyclohexane to the dicyano groups. More specifically, they have proposed an avoided crossing between the S_1 and S_2 excited states along the torsional angle (τ). According to the Verhoeven picture, the S_1 excited state lives in a weak local minimum that can radiate to the ground state, while the S_2 state undergoes an ultrafast cis−trans isomerization back to the ground state after photo-excitation. See Figure 7 in ref 32.

To simulate this putative relaxation process, we have investigated the PES of PYCM as follows. First, we performed a geometry optimization for the first excited state (S_1) at the CIS level. Although we had no confidence in the accuracy of the CIS method to generate excitation energies, we reasoned that if twisting a double bond were really a robust feature of PYCM, then CIS approach should find an optimal structure with the ethylenic groups pointed out of plane; indeed, our results confirmed such a geometry. Second, apart from the dihedral angle τ shown in Figure 1, (i.e., the dihedral angle along the cyclohexane-dicyano group double bond), we froze all the other geometrical coordinates in PYCM . At equilibrium τ is 0° . Then, we calculated the PESs along τ to learn about electronic relaxation, and we found a small barrier for the S_1 state between τ = 0° and 90°.

In Figure 2, we plot VOA-CIS energies (left-hand side) and relative dipole moments ($|\vec{\mu}_{\mathrm{rel}}| \equiv |\vec{\mu}_{\mathrm{ex}} - \vec{\mu}_{\mathrm{g}}|$, right-hand side) as a function of the torsional angle τ, for a few different VOA-CIS parameter options. We plot the first four singlet states, S_0−S_3, with S_0 being the ground state. From the dipole moment plot, one can see that the CT state $|D^+A^-\rangle$ changes its adiabatic surface as a function of τ, moving smoothly from S_1 (red) to S_2 (green) as τ goes from 0° to 90° . Conversely, the locally excited state $|DA^*\rangle$, changes its surface as well, moving smoothly from S_2 to S_1 . In Figure 3, these VOA-CIS findings are confirmed by EOM-CCSD[33] data, where we show that both methods (VOA-CIS-G(12, 2) and EOM-CCS(D) yield very similar absolute dipole moments for S_1. From the energy plot, we compute that the corresponding avoided crossing occurs when τ is around 40°. Thus, VOA-CIS captures PYCM's experimental features described above and, in the process, highlights the power of a variational method near an avoided crossing.

To underscore the importance of a variational method, we provide a comparison with CIS(D) in Figure 4a. Here, although CIS(D) finds the correct excited states in the τ = 0 and τ = 90 limits, because the method is perturbative, CIS(D) PESs and dipole moments are not smooth (and in fact, completely distorted) along the τ coordinate. In part b, we show results from SOS-CIS(D_0) the scaled-opposite version of the CIS(D_0).

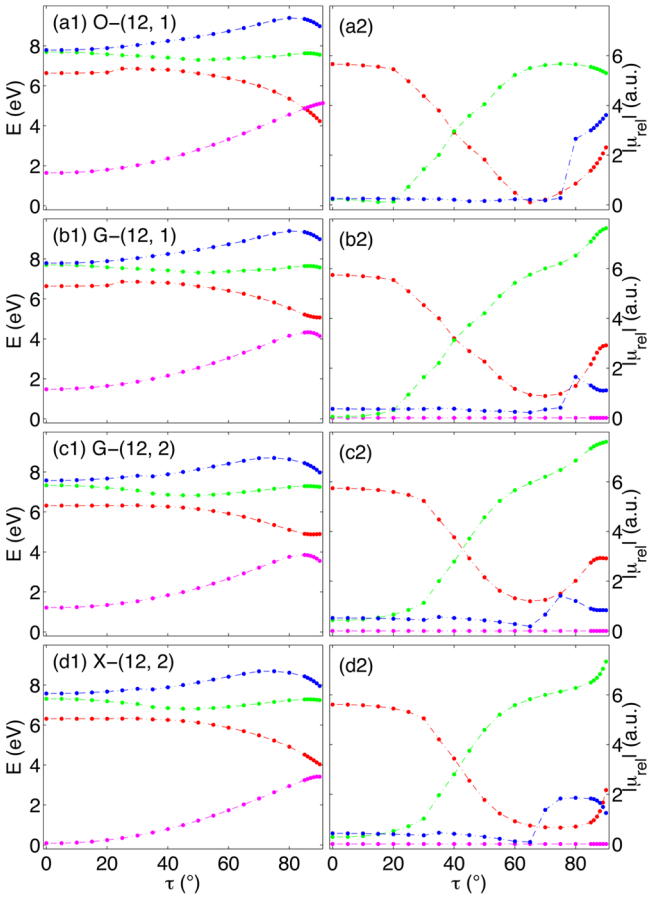

Figure 2. VOA-CIS-C(12, m) energies and corresponding dipole moments (relative to the ground state) $|\vec{\mu}_{rel}|$ as a function of torsional angle τ. The zero of energy here is the VOA-CIS-X(12, 3) energy at τ = 0. Note that in part a (VOA-CIS-O(n, m)) the ground state is not included in the basis; thus, the HF energy is used for S_0.

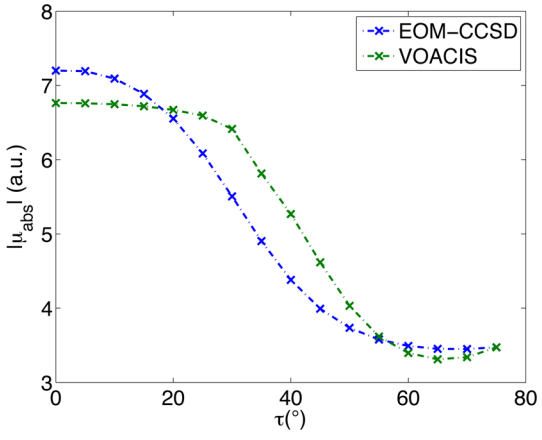

Figure 3. $|\vec{\mu}_{abs}|$ (a.u.) for S_1 as a function of torsional angle τ, for EOM-CCSD and VOA-CIS-G(12, 2) . Note that both methods find very similar geometries for the avoided crossing as a function of τ.

Recall that the CIS(D_n) suite of methods were designed to handle quasi-degenerate excited states. As expected, SOS-CIS(D_0) curves are much smoother than CIS(D) curves. However, numerically, we find that SOS-CIS(D_0) excitation energies are problematic. In particular, at the equilibrium geometry τ = 0°, which should be far away from the crossing, SOS-CIS(D_0) predicts that the $|D^+A^-\rangle$ and the $|DA^*\rangle$ diabatic

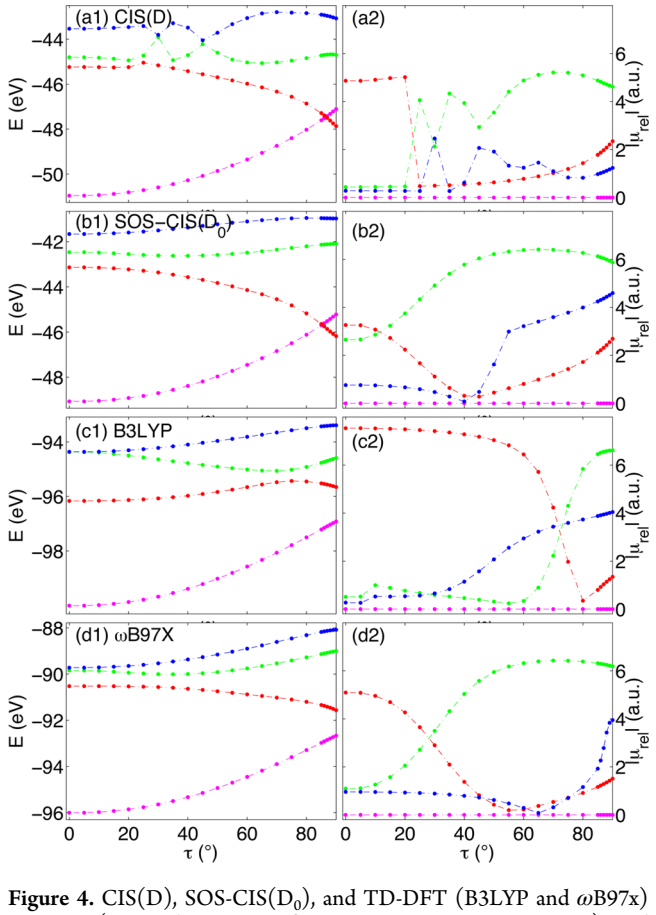

Figure 4. CIS(D), SOS-CIS(D_0), and TD-DFT (B3LYP and ωB97x) energies (using the same reference energy as in Figure 2) and corresponding dipole moments (relative to the ground state) $|\vec{\mu}_{rel}|$ as a function of torsional angle τ.

states should be strongly mixed together in the S_1 and S_2 adiabatic states, according to the dipole moments. Thus, SOS-CIS(D_0) would appear not to stabilize CT states enough; this statement is confirmed by the fact that SOS-CIS(D_0) predicts that S_1 should have a much larger oscillator strength than S_2 (more than a factor of 2). Experimentally, the exact opposite is true: S_2 is much brighter than S_1 (which is also predicted by VOA-CIS). As a side note, we showed in ref 3 that CIS(D) also does not stabilize CT states enough, though CIS(D) does better than SOS-CIS(D_0) and much better than straight CIS.

Figure 4c and d present time-dependent DFT (TD-DFT) results, using the exchange-correlation functionals B3LYP[34] and ωB97x[35] respectively. The former shows a large gap (~2 eV) for S_1 and S_2 at τ = 0°, which is significantly larger than any other method (and the experimental data, 0.88 eV as well). Moreover, the predicted crossing of diabatic states is incorrectly around 70°. These errors are likely a reflection of the well-known failure of TD-DFT for CT states[36−41] when there is no long-range correction.[35,42−53]

By including long-range exchange, ωB97x[35] performs much better than B3LYP in generating balanced CT vs non-CT excited states, and it locates an avoided crossing near 30° (in agreement with EOM-CCSD and VOA-CIS).

Finally, around τ = 90°, we found an intersection between S_1 and S_0. Avoided crossings between ground and excited states are common for systems that decay vibronically, and as for all near degeneracies, an accurate energetic description can be made only by invoking a variational electronic structure

dx.doi.org/10.1021/ct4009377 | J. Chem. Theory Comput. 2014, 10, 1004−1020

method. For PYCM, at the S_0-S_1 crossing, it is a locally excited state $|DA^*\rangle$ that is mixed together with the ground state.

For a faithful and smooth representation of a crossing, one must treat all ground and excited states on equal footing. Note, however, that all methods in Figure 4 ignore S_0-S_1 mixing and, as such, one often finds erroneous potential energy surfaces (e.g., S_0-S_1 conical intersections with the wrong topology).[54] Among the suite of VOA-CIS methods, VOA−CIS−O(n, m) has the exact same problem; in fact, VOA−CIS−O(n, m) predicts that S_1 can have a lower energy than the ground state energy E_{HF}. Fortunately, using VOA-CIS-G(n, m) or VOA-CIS-X(n, m) we can safely include the ground state wave function while barely changing with relative energies among the excited states. This fortunate state of affairs reflects the strengths of VOA-CIS as a variational method.

3. Diabatization with Boys Localization. Having calculated smooth adiabatic potential energy surfaces through the VOA-CIS algorithm, one can make a preliminary analysis of electronic relaxation processes through diabatization. In the Appendix, we briefly review Boys localization as a tool for generating localized diabatization. Using Boys localized diabatization, in Figure 5 we plot the energies and relative

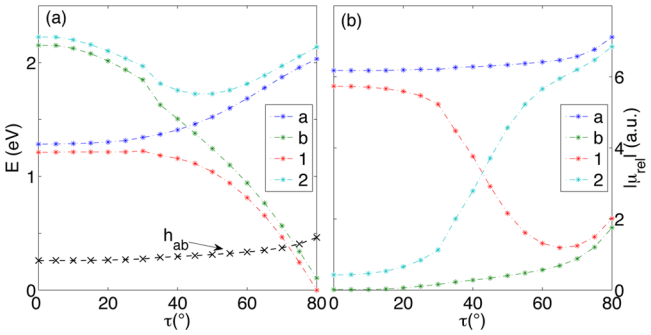

Figure 5. (a) VOA-CIS-G(12, 2) energy and (b) $|\vec{\mu}_{rel}|$ relative to the ground state, as a function of torsional angle τ, for both adiabatic (labeled as 1, 2) and diabatic (labeled as a, b) states. In part a, the diabatic coupling h_{ab} is also shown. The zero of energy here is E_1 at τ = 80°.

dipole moments from VOA-CIS-G(12, 2), for both adiabatic states (S_1 and S_2) and their corresponding diabatic states for the PYCM molecule (again, as a function of the torsional angle τ). States 1, 2 and a, b represent adiabatic and diabatic states respectively. As would be expected in an avoided crossing, the energies of diabatic states a and b do cross near τ = 40°. Moreover, in part b, the dipole moments show that diabatic state a is indeed the CT state, characterized by a large dipole moment; whereas state b is a non-CT excited state. Thus, Boys-localized diabatic VOA-CIS is in agreement with the experimentalist's picture of PYCM, and we may conclude that the VOA-CIS algorithm gives us a meaningful starting point for studying electronic relaxation.

Lastly, beyond individual surface energies, Figure 5 provides us with a plot of the diabatic coupling h_{ab} (in part a) as a function of τ. According to the Condon approximation,[55] one assume that h_{ab} is a constant at all geometries. From the figure, however, we see that h_{ab} increases smoothly with τ, so that the absolute value of h_{ab} at τ = 80° is roughly twice as big as the value at τ = 0°. This form of the diabatic coupling will be important for calculating the physical relaxation time for PYCM.

B. Benchmark Molecules. As another test of the VOA-CIS method, we study the 28 small to medium-sized molecules[56] recently benchmarked by the Thiel group. This rich set of organic test molecules includes unsaturated aliphatic hydrocarbons, aromatic hydrocarbons and heterocycles, carbonyl molecules (including aldehydes, ketones, and amides), and nucleobases. The relevant excited states are usually of valence character, though several Rydberg states are also included; nominally, all vertical excitations can be classified as either $\sigma \rightarrow \pi^*$, $\pi \rightarrow \pi^*$, or $n \rightarrow \pi^*$. In ref 56, the Thiel group provided singlet and triplet energies, as calculated by a variety of different methods, including CASPT2, CC2, CCSD, and CC3.

In this work, we have performed VOA-CIS calculation for all singlet excited states considered by Thiel et al., specifically 104 calculations. We restricted ourselves to singlets because we do not yet have operational VOA-CIS triplet code. All calculations were performed with the TZVP basis set and we used the geometries as provided in ref 56. Using the symmetry of each electronic state, we were able to compare our VOA-CIS data with all other electronic structure data in Table V in section VII.C (Appendix).

1. Method 1 for Quantifying Accuracy: Absolute Error. In order to compare VOA-CIS data quantitatively versus the Thiel benchmarked data, two different approaches seem intuitive. On the one hand, we can use the errors from the absolute excitation energies. To be precise, assume we have two sets of energies obtained from different methods, one labeled std for reference, and the other labeled trial for our new data. For the mth (m = 1, 2, ..., 28) molecule, assuming we get n_m states, then for each state j, we can define an *absolute* error for that state:

$$\mathrm{Err}_{m,j} = E_{m,j}^{\mathrm{trial}} - E_{m,j}^{\mathrm{std}} \qquad (j = 1, 2, ..., n_m)$$

With this in mind, we can estimate the overall quality of the VOA-CIS method by computing the mean value of these absolute errors for each molecule m ($\mathrm{Err}_{m,j}$):

$$\mathrm{Err}_m^{\mathrm{abs}} \equiv \frac{\sum_{j=1}^{n_m} |\mathrm{Err}_{m,j}|}{n_m} \tag{20}$$

2. Method 2 for Quantifying Accuracy: Relative Error. Beyond absolute excitation energy errors, another option is to analyze the VOA-CIS method through relative excitation energy errors. Because VOA-CIS was designed to optimize orbitals and thus rebalance relative vertical excited state energies (rather than absolute vertical energies), we might expect to see better performance for relative energies according to VOA-CIS. In fact, for a few cases, we find that VOA-CIS tends to underestimate excitation energies—for instance, in section IV.D, we will show that VOA-CIS consistently underestimates absolute vertical excitation energies of Rydberg states. Nevertheless, even with Rydberg states present, the method VOA-CIS does find much more accurate relative excited state energies than absolute excited state energies. With that in mind, we can define a simple measure of the relative error of VOA-CIS for molecule m as

$$\mathrm{Err}_m^{\mathrm{rel}} \equiv \sqrt{\frac{\sum_{i,j=1}^{n_m} (\mathrm{Err}_{m,i} - \mathrm{Err}_{m,j})^2}{{n_m}^2}} \tag{21}$$

(Since n_m can be 1, it is not convenient to define the denominator in eq 21 as n_m ($n_m - 1$) as would be standard for a variance calculation.)

dx.doi.org/10.1021/ct4009377 | J. Chem. Theory Comput. 2014, 10, 1004−1020

Notice that, if there were two sets of excitation energies with the following form,

$$x_{m,j}^{\text{trial}} = x_{m,j}^{\text{std}} + c_m, \qquad j = 1, 2, \ldots, n_m$$

then $\text{Err}_m^{\text{abs}}$ would give the overall shift $|c_m|$, while $\text{Err}_m^{\text{rel}}$ is exactly 0, according to the definitions above. For this reason, it is clear that Err^{abs} and Err^{rel} offer two important and complementary means of assessing the validity of the VOA-CIS algorithm.

3. Results. In Figures 6 and 7, we plot Err^{abs} and Err^{rel} respectively for the 28 different molecules in Thiel benchmark

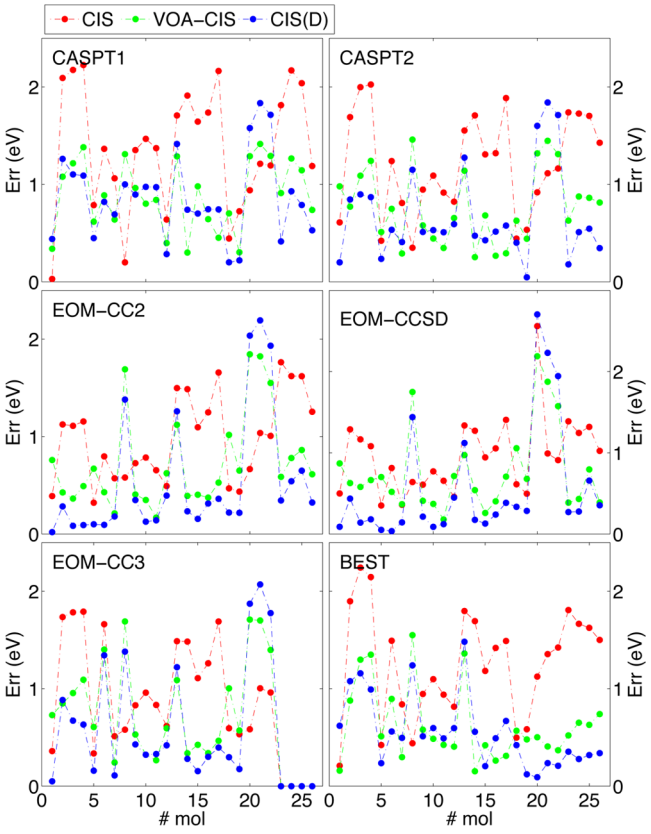

Figure 6. *Absolute* errors (Err^{abs}) of CIS, VOA-CIS-G(12, 2), and CIS(D) as compared with different "standard" methods. "Best" here refers to the numerical values which Thiel et al. have judged most accurate.[56]

set. Now unfortunately, as the Thield group emphasizes, it is not usually possible to conclude which reference method is the most accurate among the list of CC2, CC3, EOM-CCSD, CASPT2 and postprocessed experimental data. As such, in Figures 6 and 7, we compare VOA-CIS versus all possible references, and we do the same for CIS and CIS(D). Both VOA-CIS and CIS(D) vastly outperform CIS, and most of the time, VOA-CIS closely follows CIS(D), suggesting that the latter two methods are nearly comparable. While CIS(D) does perform slightly better than VOA-CIS at vertical excitation energies, this discrepancy is not very surprising: CIS(D) includes all doubles and even triples at some level of perturbation theory, while VOA-CIS includes only a small subset of the doubles space. At the same time, by being a variational method, VOA-CIS works very well far away from the ground-state geometry, where CIS(D) fails. Furthermore, the Thiel benchmark set does not include any charge transfer complexes, where CIS(D) is unreliable.[3]

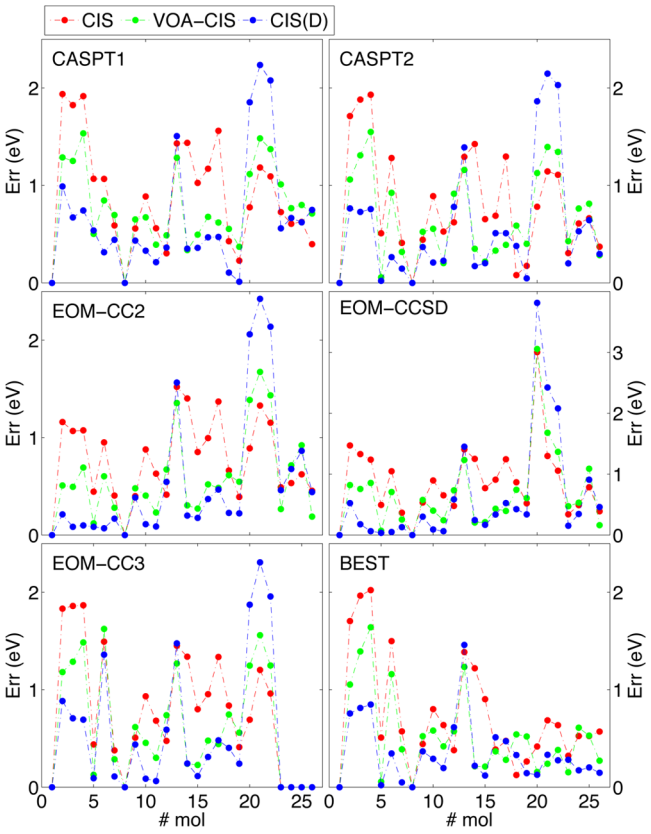

Figure 7. *Relative* errors (Err^{rel}) of CIS, VOA-CIS-G(12, 2), and CIS(D) as compared with different "standard" methods. "Best" here refers to the numerical values which Thiel et al. have judged most accurate.[56]

Future work in this arena might well benefit by further extending the basis of the VOA-CIS Hamiltonian into the triples manifold, in order to give the method additional energetic accuracy. Currently, the VOA-CIS-G Hamiltonian is very small (dimension $n^2 \times n^2$ roughly), and improvements in the VOA-CIS algorithm may well be possible with only minimal cost.

C. CH_2O. For our final two test cases, we choose small organic molecules where Rydberg states are embedded in valence states. As the reader will see, these cases present difficulties for the VOA-CIS algorithm. We begin with formaldehyde.

Because of a plethora of Rydberg states mixed with valence states, for accurate results on formaldehyde, one is forced to use a large basis replete with diffuse functions and then one must hope for a balanced measure of the energies of valence states versus Rydberg states. When using a big basis set 6-311(2+, 2+)G(d, p), EOM-CCSD almost recovers experimental data; for the standard suite of post-CIS methods out there (CIS(D), CIS(D_0), SOS-CIS(D_0)), each successive method improves on the accuracy of its predecessor.[16]

In Tables II and III, we present energies and oscillator strengths respectively, for CIS, TDHF, VOA-CIS-G(14, m) with m = 1, 2, 3, EOM-CCSD, and experimental data. Experimental state assignments are from ref 16. VOA-CIS and CIS excited states were matched up according to wave function overlap. In the case of VOA-CIS, we find that our results closely follow experimental data, with the exception of the S_1 state. For the most part, where experimental evidence is available, the

dx.doi.org/10.1021/ct4009377 | J. Chem. Theory Comput. 2014, 10, 1004−1020

Table II. Comparison of Excitation Energies for CH_2O from various ab initio methods with experimental data[a]

no.	E_{CIS}	E_{TDHF}	E_1	E_2	E_3	$E_{EOM\text{-}CCSD}$	E_{exp}	state[b]
1	4.48	4.30	3.56	3.51	3.58	3.95	4.07	V
2	8.64	8.63	7.03	7.05	7.12	7.06	7.11	R
3	9.37	9.36	7.78	7.91	7.98	7.89	7.97	V
4	9.46	9.08	8.78	8.81	8.91	10.00		R
5	9.67	9.42	8.85	9.01	9.08	8.00		R
6	9.67	9.59	7.90	8.02	8.05		8.14	V
7	9.78	9.78	8.07	8.19	8.26	8.23	8.37	R
8	10.61	10.61	8.87	9.02	9.12	9.07	8.88	R
9	10.87	10.86	9.13	9.28	9.37	9.38		R
10	10.89	10.86	9.22	9.34	9.43	9.27		R

[a]Note the almost perfect recovery of experimental data from VOA-CIS except for the first state. E_m, $m \in \{1, 2, 3\}$ corresponds to VOA-CIS-G(12, m). Nuclear geometries are optimized with MP2/6-31G* (following ref 16). EOM-CCSD and experimental data are also from ref 16. [b]Valence (V) and Rybderg (R) state assignmments are cited from ref 6.

Table III. Comparison of Oscillator Strengths for CH_2O from Various ab initio Methods[a]

#	f_{CIS}	f_{TDHF}	f_1	f_2	f_3	$f_{EOM-CCSD}$
1	0.0000	0.0000	0.0000	0.0000	0.0000	0.0000
2	0.0227	0.0216	0.0096	0.0115	0.0123	0.0160
3	0.0467	0.0456	0.0390	0.0357	0.0397	0.0376
4	0.2606	0.2219	0.1335	0.1414	0.1312	0.2217
5	0.0005	0.0003	0.0001	0.0000	0.0000	0.0482
6	0.0160	0.0203	0.0338	0.0358	0.0318	-
7	0.0000	0.0000	0.0000	0.0000	0.0000	0.0000
8	0.0143	0.0138	0.0023	0.0018	0.0023	0.0115
9	0.0023	0.0025	0.0004	0.0006	0.0000	0.0330
10	0.0059	0.0033	0.0674	0.0516	0.0417	0.0193

[a]f_m, $m \in \{1, 2, 3\}$ corresponds to VOA-CIS-G(12, m). Nuclear geometries are optimized with MP2/6-31G* (following ref 16).

difference between VOA-CIS and experiment is within 0.2 eV, much smaller than typical CIS data.

These are encouraging features of the VOA-CIS algorithm. For this problem, we find that VOA-CIS can actually address Rydberg states quite well (and with a much cheaper cost than EOM-CCSD). Nevertheless, the reader should note that VOA-CIS and EOM-CCSD oscillator strengths are quite different, often by a factor of 2.

D. C_2H_4. For our final test case, we now show a clear failure of the VOA-CIS approach: the molecule ethylene. Following the work of Martinez et al.,[57,58] many researchers have studied the photochemistry of C_2H_4; after photoexcitation, the molecule is quickly funneled through a conical intersection where it pyramidalizes while also breaking a double bond to yield a cis−trans isomerization. Ethylene photoisomerization is a prototypical model system for photochemistry.

For ethylene, even more so than formaldehyde, at many geometries the lowest-lying states are dominated by Rydberg states (rather than valence states). In fact, at the equilibrium geometry the lowest lying few states are all Rydberg states (R(3s), R(3p_x), R(3p_y), and R(3p_z)) for C_2H_4, except for one valence state $\pi \rightarrow \pi^*$.[59] For the most part, the Rydberg states were ignored by early nonadiabatic dynamics calculations[60] that focused on valence states instead; at the same time, however, the electronic structure community recognizes ethylene as a difficult test case for electronic structure precisely because of valence-Rydberg mixing.

With this in mind, we have sought to test the VOA-CIS method on ethylene, and to check whether we can find accurate potential energy surfaces. In ref 3, we reported strong results for twisted ethylene, where our results matched up well with MRCI results; but for a twisted geometry, all low-lying excited states for ethylene are valence states. In this paper, in Table IV we report results for ethylene at the ground-state geometry, where most Rydberg state compete lie energetically below any valence states.

Table IV. Comparison of Excitation Energies for C_2H_4[a]

no.	E_{CIS}	E_1	E_2	E_3	E_{exp}	state[b]
1	7.12	5.84	5.83	6.13	7.11	R (3s)
2	7.71	6.47	6.49	6.79	7.80	R (3p_y)
3	7.74	6.98	7.05	7.37	7.60	V
4	7.86	6.47	6.48	6.77	8.01	R (3p_z)
5	8.09	6.74	6.79	7.11	8.29	R (3p_x)

[a]E_m, $m \in \{1, 2, 3\}$ corresponds to VOA-CIS-G(12, m). Nuclear geometries are optimized with MP2/6-31G* (following ref 16). Experimental data is also from ref 16. [b]Valence (V) and Rydberg (R) state assignments are cited from ref 59.

Unfortunately, from Table IV, we find that the VOA-CIS method does poorly in this case. In particular, we find that Rydberg states are strongly stabilized by the VOA-CIS method, while (perhaps unsurprisingly) the ground state does not gain much correlation energy by orbital relaxation of Rydberg states. As a result, the VOA-CIS vertical excitation energies in Table IV are all too low (by 1.0 to 1.5 eV). Even the CIS results agree much better with the experiment than VOA-CIS . Lastly, and worst of all, VOA-CIS does not find the correct relative energies for this example. Over all, this molecule highlights that VOA-CIS is not a good option for electronic structure problems dominated by Rydberg states. Luckily, our interest is in condensed phase chemistry, and Michl has argued convincingly that Rydberg states will not be important in most solvents.[61]

V. DISCUSSION

Having demonstrated the strengths of the VOA-CIS algorithm (as well as its limitations), we now want to address two subtle points about how the VOA-CIS algorithm works, which may also give insight into its performance.

A. Visualizing the θ Matrix for Orbital Relaxation. The VOA-CIS algorithm finds an improved balance between CT and non-CT excited states via orbital relaxation. To that end, one can ask a very simple question: what is the nature of that

orbital relaxation for the case of a CT excited state? To answer this question, in Figure 8, we visualize the attachment−

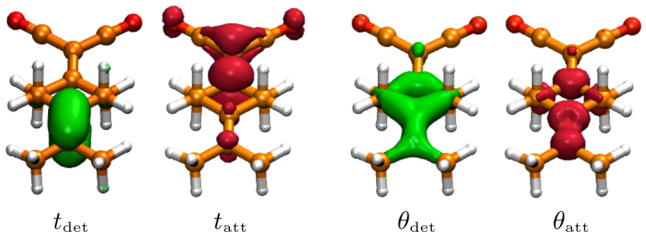

Figure 8. Detachment and attachment plots of t and θ for the CT state for PYCM.

detachment densities[1] of the t matrix, together with the *normalized* θ^{II}_{ai} matrix associated with a CT CIS state ($|\Psi^{I}_{CIS}\rangle$). In other words, for the latter we consider the electronic density of the state $|\Psi\rangle = \sum_{ai}\theta^{II}_{ai}a^{\dagger}_{a}a_{i}|\Phi_{HF}\rangle$. In analogy with standard CIS densities, the attachment−detachment densities for θ^{II}_{ai} are

$$D^{det}_{ij} = \sum_{a}\theta^{II}_{ai}\theta^{II}_{aj} \tag{22}$$

$$A^{att}_{ab} = \sum_{i}\theta^{II}_{ai}\theta^{II}_{bi} \tag{23}$$

From Figure 8, one can easily infer that, in the case of a CT excited state, according to VOA-CIS, orbital relaxation remains entirely local. Thus, even though a CT state is characterized by one bare electron moving a long distance from detachment to attachment, VOA-CIS predicts that the subsequent energetic drop in energy caused by electron−electron correlation is due to local orbital relaxation. This local nature of electronic shielding is consistent with the simple He_2 example studied in ref 2 and suggests that local correlation approaches[62] on top of CIS might even be possible.

B. Relationship with TDHF. In broad terms, the VOA-CIS X option stipulates that, by considering the set of CIS states, one can introduce wave functions into the electronic basis that help to capture the dynamical correlation of the ground state. For the sophisticated quantum chemist, this language bears the signature of TDHF, and indeed, there is a close connection between TDHF and the VOA-CIS-X(n, m) algorithm. We will now demonstrate as much.

Using the language of ref 5 for this section only, the TDHF[4,5] excitation energies and quasi-wave functions are defined via

$$\begin{pmatrix}\mathbf{A} & \mathbf{B}\\ \mathbf{B}^{*} & \mathbf{A}^{*}\end{pmatrix}\begin{pmatrix}\mathbf{X}\\ \mathbf{Y}\end{pmatrix} = \omega\begin{pmatrix}1 & 0\\ 0 & -1\end{pmatrix}\begin{pmatrix}\mathbf{X}\\ \mathbf{Y}\end{pmatrix} \tag{24}$$

in which $\omega = E_{CIS} - E_{HF}$ is the excitation energy, and the corresponding matrix elements are

$$\mathbf{A}_{ia,jb} = \delta_{ij}\delta_{ab}(\varepsilon_{a} - \varepsilon_{i}) + \langle aj||ib\rangle$$

$$\mathbf{B}_{ia,jb} = \langle ab||ij\rangle \tag{25}$$

Now, let us write out eq 24 as two separate equations:

$$\begin{cases}\mathbf{AX} + \mathbf{BY} = \omega\mathbf{X}\\ \mathbf{B}^{*}\mathbf{X} + \mathbf{A}^{*}\mathbf{Y} = -\omega\mathbf{Y}\end{cases} \tag{26}$$

Setting $\mathbf{B} = 0$ corresponds to standard CIS theory (or the Tamm-Dancoff approximation for TD-DFT).

If we now stipulate that the **B** matrix should be a first-order perturbation in the Hamiltonian relative to CIS, while the **Y** vector should be the first-order correction to the wave function, we notice that, in eq 26, the first equation is second-order in **Y**, while the second one is first-order in **Y**. At this point, one can solve for **Y** in a straightforward manner via perturbation theory. If one further approximates that **A** is diagonally dominant when computing the $\mathbf{A}^{-1}$ matrix, one arrives at the final form:

$$Y_{ai} \approx -\sum_{bj}\frac{\langle ab||ij\rangle X_{bj}}{\omega + \varepsilon_{a} - \varepsilon_{i}} = -\frac{\langle\Phi_{HF}|Ha^{\dagger}_{a}a_{i}|\Psi_{CIS}\rangle}{\varepsilon_{a} - \varepsilon_{i} + E_{CIS} - E_{HF}} \tag{27}$$

Equation 27 is identical to eq 8 (up to a constant factor). This connection is a strong endorsement of our VOA-CIS algorithm. The usual interpretation of the **Y** is a "de-excitation" of the ground state relative to a singles wave function, or in other words, a doubly excited contribution to the ground-state. Thus, it would appear that the VOA-CIS algorithm is an extension of TDHF to include the electron−electron correlations that excited states inflict on each other (not just on the ground state). In the future, it would be interesting to compare the ground-state correlation energy produced by VOA-CIS-X(n, m) with the TDHF (or RPA) correlation energy.

VI. CONCLUSIONS AND FUTURE DIRECTIONS

In this article, we have presented the VOA-CIS algorithm and benchmarked its performance across a series of interesting photoexcitable organic molecules. VOA-CIS is a variational post-CIS electronic structure theory method that generates smooth and (usually) accurate potential energy surfaces; it works well for isolated energies or when there are degeneracies present. The method will not work well for molecules where Rydberg states dominate the excited state spectrum. The essential input for the VOA-CIS algorithm is the number of CIS states requested n; otherwise, the algorithm can be viewed as a blackbox approach. In many cases, VOA-CIS achieves energetic accuracy comparable to much more expensive methods and with a much cheaper cost.

Looking forward, our next goals in developing the VOA-CIS algorithm are threefold. (1) We plan to optimize our VOA-CIS code and implement a completely parallelizable algorithm. (2) We will explore the possibilities of incorporating triple excitations into the VOA-CIS algorithm for extra accuracy. (3) We will develop analytic gradients and derivative coupling for VOA-CIS . In the end, we believe the VOA-CIS algorithm can become a robust algorithm for studying electronic relaxation in almost all organic chromophores.

VII. APPENDIX

A. Localized Diabatic States

For photo-excited systems undergoing electron or energy transfer processes, the initial and final states pre-transfer are not always adiabatic states ($\{|\Phi_{J}\rangle, J = 1, 2, ...\}$). Recall that, by definition, adiabatic states are the eigenvectors produced by diagonalizing the molecular electronic Hamiltonian at a given nuclear geometry. In a condensed phase system, however, solvent is often ignored which can lead to unstable adiabatic electronic states. Moreover, the derivative couplings to nuclear motion can be significant, and thus lead to a complete failure of the Born−Oppenheimer approximation. For both of these

dx.doi.org/10.1021/ct4009377 | J. Chem. Theory Comput. 2014, 10, 1004−1020

Table V. Comparison of VOA-CIS Energies with Results from Other Excited-State Approaches[a]

name	no. mol	no. S	no. CIS	no. VOA-CIS	CASPT2	CASPT2	CC2	CCSD	CC3	best	E_{CIS}	$E_{VOA-CIS}$
ethene	0	0	0	1	7.98	8.62	8.40	8.51	8.37	7.80	8.01	7.64
E-butadiene	1	0	0	0	6.23	6.47	6.49	6.72	6.58	6.18	6.44	5.90
	1	1	6	3	6.27	6.83	7.63	7.42	6.77	6.55	9.22	7.76
all-*E*-hexatriene	2	0	0	0	5.01	5.31	5.41	5.72	5.58	5.10	5.47	4.96
	2	1	6	2	5.20	5.42	6.67	6.61	5.72	5.09	8.24	6.92
all-*E*-octatetraene	3	0	3	1	4.38	4.64	5.87	5.99	4.97	4.47	7.50	6.32
	3	1	0	0	4.42	4.70	4.72	5.07	4.94	4.66	4.83	4.19
cyclopropene	4	0	1	0	6.36	6.76	6.96	6.96	6.90	6.76	7.34	6.21
	4	1	0	1	7.45	7.06	7.17	7.24	7.10	7.06	6.92	6.59
cyclopentadiene	5	0	0	0	5.27	5.51	5.69	5.87	5.73	5.55	5.54	5.09
	5	1	3	3	6.31	6.31	7.05	7.05	6.61	6.31	8.42	7.49
	5	2	5	9	7.89	8.52	8.86	8.95	6.69	–	8.92	8.86
norbornadiene	6	0	0	0	5.28	5.34	5.57	5.80	5.64	5.34	5.67	5.18
	6	1	1	1	6.20	6.11	6.37	6.69	6.49	6.11	7.25	6.50
	6	2	3	5	6.48	7.32	7.65	7.87	7.64	–	8.04	7.70
	6	3	4	4	7.36	7.44	7.66	7.87	7.71	–	8.27	7.57
benzene	7	1	0	0	6.30	6.45	6.68	6.74	6.68	6.54	6.10	4.99
naphthalene	8	0	1	1	4.03	4.24	4.45	4.41	4.27	4.24	5.24	4.70
	8	1	0	0	4.56	4.77	4.96	5.21	5.03	4.77	5.09	4.50
	8	2	5	6	5.39	5.90	6.22	6.23	5.98	5.90	7.34	6.96
	8	3	2	2	5.53	6.00	6.21	6.53	6.07	6.00	6.77	6.42
	8	3	2	4	5.53	6.00	6.21	6.53	6.07	6.00	6.77	6.69
	8	4	3	3	5.54	6.07	6.25	6.55	6.33	6.07	7.08	6.44
	8	6	4	5	5.93	6.33	6.57	6.77	6.57	6.33	7.27	6.72
furan	9	0	0	0	6.04	6.43	6.75	6.80	6.60	6.32	6.53	6.26
	9	1	2	1	6.16	6.52	6.87	6.89	6.62	6.57	8.16	6.57
	9	2	7	7	7.66	8.22	8.78	8.83	8.53	8.13	9.15	8.97
pyrrole	10	0	2	1	5.92	6.31	6.61	6.61	6.40	6.37	7.65	6.43
	10	1	0	2	6.00	6.33	6.83	6.87	6.71	6.57	6.78	6.70
	10	2	8	8	7.46	8.17	8.44	8.44	8.17	7.91	8.89	8.63
imidazole	11	0	1	0	6.52	6.81	6.86	7.01	6.82	6.81	7.21	6.23
	11	1	0	1	6.72	6.19	6.73	6.80	6.58	6.19	7.07	6.52
	11	2	3	3	7.15	6.93	7.28	7.27	7.10	6.93	7.96	7.15
	11	3	2	2	7.56	7.91	8.00	8.15	7.93	–	7.90	6.79
	11	4	9	9	8.51	8.15	8.62	8.70	8.45	–	9.33	8.78
pyridine	12	0	1	1	4.84	5.02	5.32	5.27	5.15	4.85	6.19	5.48
	12	1	0	0	4.91	5.14	5.12	5.25	5.05	4.59	6.13	5.44
	12	2	6	6	5.17	5.47	5.39	5.73	5.50	5.11	8.61	8.08
	12	3	2	3	6.42	6.39	6.88	6.94	6.85	6.26	6.51	6.68
	12	4	4	5	7.23	7.46	7.72	7.94	7.70	7.18	8.42	7.99
	12	5	5	4	7.48	7.29	7.61	7.81	7.59	7.27	8.44	7.86
pyrazine	13	0	0	0	3.63	4.12	4.26	4.42	4.24	3.95	5.13	4.01
	13	1	4	2	4.52	4.70	4.95	5.29	5.05	4.81	7.03	4.92
	13	2	1	1	4.75	4.85	5.13	5.14	5.02	4.64	5.98	4.76
	13	3	3	3	5.17	5.68	5.92	6.02	5.74	5.56	6.70	5.35
	13	4	11	5	6.13	6.41	6.70	7.13	6.75	6.60	9.81	6.58
	13	5	2	4	6.70	6.89	7.10	7.18	7.07	6.58	6.65	6.37
	13	6	5	6	7.57	7.79	8.13	8.34	8.06	7.72	8.75	7.80
	13	7	6	7	7.70	7.65	8.07	8.29	8.05	7.60	9.07	7.85
pyrimidine	14	0	0	0	3.81	4.44	4.49	4.70	4.50	4.55	5.87	4.88
	14	1	2	1	4.12	4.81	4.84	5.12	4.93	4.91	6.56	5.52
	14	2	1	2	4.93	5.24	5.51	5.49	5.36	5.44	6.50	5.87
	14	3	3	4	6.72	6.64	7.12	7.17	7.06	6.95	6.90	7.15
	14	4	7	7	7.32	7.64	8.08	8.24	8.01	–	8.88	8.48
	14	5	6	6	7.57	7.21	7.79	7.97	7.74	–	8.61	8.06
pyridazine	15	0	0	0	3.48	3.78	3.90	4.11	3.92	3.78	4.91	3.59
	15	1	1	1	3.66	4.32	4.40	4.76	4.49	4.32	6.10	4.78
	15	2	2	2	4.86	5.18	5.37	5.35	5.22	5.18	6.32	5.24
	15	3	4	3	5.09	5.77	5.81	6.00	5.74	5.77	7.29	5.61
	15	4	6	5	5.80	6.52	6.40	6.70	6.41	–	8.43	7.00
	15	5	3	4	6.61	6.31	7.00	7.09	6.93	–	6.56	6.34

dx.doi.org/10.1021/ct4009377 | J. Chem. Theory Comput. 2014, 10, 1004−1020

Table V. continued

name	no. mol	no. S	no. CIS	no. VOA-CIS	CASPT2	CASPT2	CC2	CCSD	CC3	best	E_{CIS}	$E_{VOA-CIS}$
	15	6	5	6	7.39	7.29	7.57	7.79	7.55	–	8.32	7.43
	15	7	7	7	7.50	7.62	7.90	8.11	7.82	–	8.67	7.83
s-tetrazine	17	0	0	0	1.96	2.24	2.47	2.71	2.53	2.24	3.52	1.83
	17	1	1	1	3.06	3.48	3.67	4.07	3.79	3.48	5.67	3.61
	17	2	2	2	4.51	4.73	5.10	5.32	4.97	4.73	6.08	4.53
	17	3	3	4	4.89	4.91	5.20	5.27	5.12	4.91	6.24	4.76
	17	4	4	3	5.05	5.18	5.53	5.70	5.34	5.18	6.56	4.72
	17	6	5	5	5.28	5.47	5.50	5.70	5.46	5.47	6.65	5.12
	17	7	9	6	5.48	6.07	6.32	6.76	6.23	–	9.36	6.12
	17	8	11	8	5.99	6.38	6.91	7.25	6.87	–	9.79	6.77
	17	10	8	9	6.37	6.77	6.70	6.99	6.67	–	8.68	6.97
	17	11	6	7	7.13	6.96	7.60	7.66	7.45	–	6.88	6.52
	17	12	7	10	7.54	7.43	7.75	8.06	7.79	–	8.58	7.28
	17	13	10	11	7.94	8.15	8.65	8.88	8.51	–	9.53	8.35
formaldehyde	18	0	0	0	3.91	3.98	4.09	3.97	3.95	3.88	4.46	2.93
	18	1	1	2	9.09	9.14	9.35	9.26	9.18	9.10	9.62	9.04
	18	2	2	3	9.77	9.31	10.34	10.54	10.45	9.30	9.67	9.05
acetone	19	0	0	0	4.18	4.42	4.52	4.43	4.40	4.40	5.10	3.78
	19	1	3	3	9.10	9.27	9.29	9.26	9.17	9.10	9.77	9.31
	19	2	2	2	9.16	9.31	9.74	9.87	9.65	9.40	9.69	8.89
formamide	21	0	0	0	5.61	5.63	5.76	5.66	5.65	5.63	6.42	5.25
	21	1	2	1	7.41	7.44	8.15	4.52	8.27	7.44	8.82	6.84
	21	2	4	3	10.50	10.54	11.24	11.34	10.93	–	10.57	8.37
acetamide	22	0	0	0	5.54	5.80	5.77	5.71	5.69	5.80	6.58	5.26
	22	1	2	2	7.21	7.27	7.66	7.85	7.67	7.27	9.02	7.07
	22	2	4	3	10.08	10.09	10.71	10.77	10.50	–	9.86	7.65
propanamide	23	0	0	0	5.48	5.72	5.78	5.74	5.72	5.72	6.62	5.20
	23	1	2	2	7.28	7.20	7.56	7.80	7.62	7.20	9.00	7.22
	23	2	4	3	9.95	9.94	10.33	10.34	10.06	–	9.82	7.73
cytosine	24	0	0	0	4.39	4.68	4.80	4.98	–	4.66	6.07	5.26
	24	1	1	1	5.00	5.12	5.13	5.45	–	4.87	6.85	5.39
	24	2	2	2	6.53	5.54	5.01	5.99	–	5.26	7.21	5.59
	24	3	3	3	5.36	5.54	5.71	5.95	–	5.62	7.45	6.21
	24	4	5	6	6.16	6.40	6.65	6.81	–	–	7.99	7.30
	24	5	10	9	6.74	6.98	6.94	7.23	–	–	9.04	7.82
thymine	25	0	0	0	4.39	4.94	4.94	5.14	–	4.82	6.23	4.80
	25	1	1	1	4.88	5.06	5.39	5.60	–	5.20	6.31	5.88
	25	2	4	4	5.88	6.15	6.46	6.78	–	6.27	8.24	7.17
	25	3	3	2	5.91	6.38	6.33	6.57	–	6.16	7.67	6.12
	25	4	6	5	6.10	6.52	6.80	7.05	–	6.53	8.65	7.45
	25	5	7	6	6.15	6.86	6.73	7.67	–	–	8.88	8.09
	25	6	5	7	6.70	7.43	7.18	7.87	–	–	8.58	8.15
	25	7	8	8	7.13	7.43	7.71	7.90	–	–	9.59	8.63
uracil	26	0	0	0	4.54	4.90	4.91	5.11	–	4.80	6.22	4.81
	26	1	1	1	5.00	5.23	5.52	5.70	–	5.35	6.49	6.03
	26	2	4	4	5.82	6.15	6.43	6.76	–	6.26	8.36	7.16
	26	3	2	2	6.00	6.27	6.73	7.68	–	6.10	7.61	6.09
	26	4	3	3	6.37	6.97	6.26	6.50	–	6.56	7.82	7.13
	26	5	5	5	6.46	6.75	6.96	7.19	–	6.70	8.76	7.58
	26	6	7	8	6.95	7.28	7.12	7.74	–	–	9.33	8.83
	26	7	8	7	7.00	7.42	7.66	7.81	–	–	9.47	8.48
adenine	27	0	0	0	5.13	5.20	5.28	5.37	–	5.25	6.23	5.76
	27	1	1	2	5.20	5.30	5.42	5.61	–	5.25	6.37	5.89
	27	2	2	1	6.15	5.21	5.27	5.58	–	5.12	7.05	5.80
	27	3	4	3	6.86	5.97	5.91	6.19	–	5.75	7.50	6.78
	27	4	5	7	6.24	6.35	6.58	6.83	–	–	7.69	7.28
	27	5	8	8	6.72	6.64	6.93	7.17	–	–	8.16	7.55
	27	6	10	10	6.99	6.88	7.49	7.72	–	–	8.37	8.01

[a]Benchmark molecules and reference data taken from ref 56. Best refers to the data which Thiel et al estimated to be the most reliable.

reasons, the adiabatic states from an electronic structure calculation may not be meaningful.

As an alternative to adiabatic states, diabatic states ($\{|\Xi_A\rangle, A = 1, 2, ...\}$) are electronic states with zero coupling to the nuclear motion; and for many circumstances, diabatic states are appropriate initial and final electronic states for chemical dynamics (e.g., when Marcus theory[55] applies). Even though the constraint of zero derivative coupling may be impossible to achieve,[64] the notion of nearly diabatic states is very helpful in quantum chemistry and has a very rich history.[65−67]

Localized diabatization is one tool to generate nearly diabatic states, and the motivation of localized diabatization is to construct the electronic states that function as the initial and final states of electron and energy transfer processes. In brief, to generate a set of localized diabatic states, one rotates together a set of adiabatic states, via a unitary transformation $\mathbf{U}_{JA}$:

$$|\Xi_A\rangle = \sum_J |\Phi_J\rangle \mathbf{U}_{JA}$$

All localized diabatization techniques are defined via a rotation matrix $\mathbf{U}$. Current available methods are generalized Mulliken Hush (GMH),[68] fragment charge difference (FCD),[69] fragment energy difference (FED),[70−72] constrained DFT (CDFT),[73] Boys localization,[74] and ER localization.[77] For a review of localized diabatization and the implicit assumptions therein, see ref 74.

In this paper, section IV.A.3, we invoke Boys localization, which is a computationally cheap generalization of the Cave/Newton GMH approach.[68] The physical motivation for the Boys algorithm is that, for CT systems, charges are stabilized and localized by a linear electric field from some solvent molecule or other auxiliary field. In practice, just like Boys localization of orbitals,[77−79] Boys localized diabatization suggests that diabatic charge centers should be as far apart as possible, thereby maximizing the quantity below:

$$f_{\text{Boys}}(\mathbf{U}) = f_{\text{Boys}}(\{\Xi_A\}) \equiv \sum_{AB} |\langle \Xi_A|\vec{\mu}|\Xi_A\rangle - \langle \Xi_B|\vec{\mu}|\Xi_B\rangle|^2 \tag{28}$$

Boys localized diabatic states indeed have very small derivative couplings.[75,76]

B. Matrix Elements from Second Quantization

For completeness, we now give the formula for the doubles−doubles block of the VOA-CIS algorithm. Equation 29 can be used to derive eq 17 in the text above.

$$\begin{aligned}
\langle \Psi^I_{\text{CIS}}|a_j^\dagger a_b \hat{H} a_a^\dagger a_i|\Psi^J_{\text{CIS}}\rangle = {} & t_l^{dI}\langle \Phi_l^{dI}|a_j^\dagger a_b \hat{H} a_a^\dagger a_i|\Phi_k^{cJ}\rangle t_k^{cJ} = \\
& +\delta_{ab}\delta_{ij}t_k^{cI}t_k^{cJ}E_{\text{HF}} \quad -\delta_{ab}t_i^{cI}t_j^{cJ}E_{\text{HF}} \quad -\delta_{ij}t_k^{aI}t_k^{bJ}E_{\text{HF}} \quad +t_i^{aI}t_j^{bJ}E_{\text{HF}} \quad +\delta_{ab}\delta_{ij}t_k^{dI}t_k^{cJ}f_{dc} \quad -\delta_{ab}\delta_{ij}t_l^{cI}t_k^{cJ}f_{kl} \\
& +\delta_{ab}t_i^{cI}t_k^{cJ}f_{kj} \quad -\delta_{ab}t_i^{dI}t_j^{cJ}f_{dc} \quad -\delta_{ab}t_k^{cI}t_k^{cJ}f_{ij} \quad +\delta_{ab}t_l^{cI}t_j^{cJ}f_{il} \\
& -\delta_{ij}t_k^{aI}t_k^{cJ}f_{bc} \quad +\delta_{ij}t_k^{cI}t_k^{cJ}f_{ba} \quad -\delta_{ij}t_k^{dI}t_k^{bJ}f_{da} \quad +\delta_{ij}t_l^{aI}t_k^{bJ}f_{kl} \\
& +t_i^{aI}t_j^{cJ}f_{bc} \quad -t_i^{aI}t_k^{bJ}f_{kj} \quad -t_i^{cI}t_j^{cJ}f_{ba} \quad +t_i^{dI}t_j^{bJ}f_{da} \quad +t_k^{aI}t_k^{bJ}f_{ij} \quad -t_l^{aI}t_j^{bJ}f_{il} \\
& +\delta_{ab}\delta_{ij}t_l^{dI}t_k^{cJ}\langle dk||lc\rangle \quad +\delta_{ab}t_i^{dI}t_k^{cJ}\langle dk||cj\rangle \quad +\delta_{ab}t_k^{dI}t_k^{cJ}\langle di||jc\rangle \quad +\delta_{ab}t_l^{cI}t_k^{cJ}\langle ik||jl\rangle \quad +\delta_{ab}t_l^{dI}t_j^{cJ}\langle di||cl\rangle \\
& +\delta_{ij}t_k^{dI}t_k^{cJ}\langle bd||ac\rangle \quad +\delta_{ij}t_l^{aI}t_k^{cJ}\langle bk||cl\rangle \quad +\delta_{ij}t_l^{cI}t_k^{cJ}\langle bk||la\rangle \quad +\delta_{ij}t_l^{dI}t_k^{bJ}\langle dk||al\rangle \\
& +t_i^{aI}t_k^{cJ}\langle bk||jc\rangle \quad +t_i^{cI}t_k^{cJ}\langle bk||aj\rangle \quad +t_i^{dI}t_j^{cJ}\langle bd||ca\rangle \quad +t_i^{dI}t_k^{bJ}\langle dk||ja\rangle \quad +t_k^{aI}t_k^{cJ}\langle bi||cj\rangle \quad +t_k^{cI}t_k^{cJ}\langle bi||ja\rangle \\
& +t_k^{dI}t_k^{bJ}\langle di||aj\rangle \quad +t_l^{aI}t_j^{cJ}\langle bi||lc\rangle \quad +t_l^{aI}t_k^{bJ}\langle ik||lj\rangle \quad +t_l^{cI}t_j^{cJ}\langle bi||al\rangle \quad +t_l^{dI}t_j^{bJ}\langle di||la\rangle
\end{aligned} \tag{29}$$

C. Table for Benchmark Molecules

In Table V, we list the individual excited state energies that were calculated and averaged together to make up Figures 6 and 7. Twenty-eight molecules are included in the benchmark set of Thiel et al.

D. Size-Consistency of VOA-CIS Method

In the text above, we claimed that the VOA-CIS algorithm provided a size-consistent approach provided that the ground-state was not included in the rediagonalized Hamiltonian. To show this, we will now demonstrate explicitly that VOA-CIS-O(n, m) (m = 1, 2) is size-consistent. In other words, suppose that we are given two molecular fragments A and B that are infinitely far away from each other in space. For an excitation on fragment A, we must prove that $E^{\text{AB}}(\text{A}^*) = E^{\text{A}}(\text{A}^*)$, where "AB" signifies a calculation with both fragments included and "A" signifies a calculation with only the one fragment.

To prove this statement, consider the AB calculation. Note that there can be no charge transfer excited states between fragments A and B because of their infinite separation. Let I and J be local excitations on A and B respectively. According to eq 5, we then find that θ^{IJ} (which is proportional to Y^{IJ}) will be 0: this follows because all interfragment two-electron integrals must vanish. θ^{IJ}_{ai} can be nonzero only if excitations I, J are located on the same fragment (say A), and the molecular orbitals a, i are also localized to that same fragment (A).

Now, for the m = 1, 2 options, all doubly excited wavefunctions have the form $|\Psi^{IJJ}\rangle = -\sum_{bj}\theta^{IJ}_{bj}a_b^\dagger a_j|\Psi^J_{\text{CIS}}\rangle$. Thus, all doubly excited configurations require that *both* excitations be on the same fragment (again, A). Finally, note that in the Hamiltonian to be rediagonalized, localized excitations on A and B cannot couple to each other at all—either directly or indirectly (because we have removed the ground-state). From this logic, we may conclude that excited states on A will not mix with excited states on B, and thus, we must have $E^{\text{AB}}(\text{A}^*) = E^{\text{A}}(\text{A}^*)$, i.e. size-consistent excitation energies.

One final word is necessary about size-consistency. For the m = 3 option, the doubly-excited configurations have the form: $|\Psi^{IJK}\rangle = -\sum_{bj}\theta^{IJ}_{bj}a_b^\dagger a_j|\Psi^K_{\text{CIS}}\rangle$. In this case, one does allow for the

possibility of excitations on both fragments, since CIS state K could be localized to fragment B, while CIS states I, J could be localized to fragment A. Nevertheless, it is easy enough to show that, after diagonalizing the Hamiltonian, we will find three distinct and nonmixing classes of excited states: those with excitations exclusively on A, those with excitations exclusively on B, and those with excitations on both A and B. The first two sets will have size-consistent energies and be meaningful. This situation is the exact scenario described in section II.D above.

E. Connection to Multireference Configuration Interaction and Neese's Spectroscopy Orientied Configuration Interaction

In section II.D above, we discussed the limitations of bare CISD. Of course, there are many effective multi-reference CI (MRCI) approaches towards generating excited states that outperform CISD and generate strong absolute and relative excitation energies.[80] While such MRCI methods are not post-CIS approaches, in general MRCI algorithms are very powerful techniques (though often expensive). Recently, Neese has proposed a spectroscopy oriented configuration interaction approach (SORCI) to excited states built on top of a CASSCF calculation for treating large molecules. At the heart of the SORCI algorithm, working in a meaningful set of average natural orbitals, the SORCI algorithm prescribes: (i) one perform a CASSCF calculation, (ii) one truncates the CASSCF wavefunctions to a smaller set of reference configurations, (iii) one generates excitations into a predefined strongly interacting subspace, and (iv) finally one rediagonalizes the Hamiltonian. (A perturbative correction for dynamic correlation is also added.) Using SORCI, one can generate quite accurate excited states for a very broad variety of molecules, small and large, for small enough configuration interactions. Nevertheless, the caveat for SORCI is that one must first choose an active space for CASSCF and second invoke several thresholds for choosing average natural orbitals, truncating the relevant reference states, and defining a strongly interacting subspace. For these reasons, the method is not "black box."

In the end, Neese's SORCI approach can *not* be mapped onto the model we propose in this manuscript (if we replace a CASSCF calculation by a CIS calculation). The reasoning is as follows. The VOA-CIS approach generates a set of doubly excited configurations in the form of a linear combination via perturbation theory. By contrast, SORCI performs no such contraction; instead, SORCI uses one threshold to generate a set of truncated reference states and a second threshold to generate a strongly interacting subspace. Thus, SORCI requires the diagonalization of a matrix of dynamic size (depending on thresholds); whereas, VOA-CIS requires the diagonalization of a matrix of static size. In general, for reasonable thresholds, we can expect that VOA-CIS will be less accurate but also significantly less expensive than a typical SORCI calculation.

AUTHOR INFORMATION

Corresponding Author

*Electronic address: subotnik@sas.upenn.edu.

Notes

The authors declare no competing financial interest.

ACKNOWLEDGMENTS

We would like to thank Qi Ou for providing helpful CISD and EOM-CCSD calculations in GAMESS.[63] We thank Anthony Dutoi and Garnet Chan for helpful conversations. This work was supported by National Science Foundation CAREER Grant CHE-1150851; J.E.S. also acknowledges an Alfred P. Sloan Research Fellowship and a David and Lucille Packard Fellowship.

REFERENCES

(1) Head-Gordon, M.; Graña, A. M.; Maurice, D.; White, C. A. *J. Phys. Chem.* **1995**, *99*, 14261−14270.
(2) Subotnik, J. E. *J. Chem. Phys.* **2011**, *135*, 071104−071104.
(3) Liu, X.; Ou, Q.; Alguire, E.; Subotnik, J. E. *J. Chem. Phys.* **2013**, *138*, 221105−221105.
(4) Mclachlan, A. D.; Ball, M. A. *Rev. Mod. Phys.* **1964**, *36*, 844−855.
(5) Dreuw, A.; Head-Gordon, M. *Chem. Rev.* **2005**, *105*, 4009−4037.
(6) Head-Gordon, M.; Rico, R. J.; Oumi, M.; Lee, T. J. *Chem. Phys. Lett.* **1994**, *219*, 21−29.
(7) Foresman, J. B.; Head-Gordon, M.; Pople, J. A.; Frisch, M. J. *J. Phys. Chem.* **1992**, *96*, 135−149.
(8) Vahtras, O.; Almlöf, J.; Feyereisen, M. W. *Chem. Phys. Lett.* **1993**, *213*, 514−518.
(9) Feyereisen, M.; Fitzgerald, G.; Komornicki, A. *Chem. Phys. Lett.* **1993**, *208*, 359−363.
(10) Helmich, B.; Hattig, C. *J. Chem. Phys.* **2011**, *135*, 214106−214106.
(11) Marcus, R. A. *J. Phys. Chem.* **1963**, *67*, 853−857.
(12) Marcus, R. A.; Sutin, N. *Biochim. Biophys. Acta* **1985**, *811*, 265−322.
(13) Head-Gordon, M.; Oumi, M.; Maurice, D. *Mol. Phys.* **1999**, *96*, 593−602.
(14) Hattig, C. *Adv. Quantum Chem.* **2005**, *50*, 37−60.
(15) Christiansen, O.; Koch, H.; Jorgensen, P. *Chem. Phys. Lett.* **1995**, *243*, 409−418.
(16) Casanova, D.; Rhee, Y. M.; Head-Gordon, M. *J. Chem. Phys.* **2008**, *128*, 164106−164106.
(17) Kats, D.; Korona, T.; Schutz, M. *J. Chem. Phys.* **2006**, *125*, 104106−104106.
(18) Helmich, B.; Hattig, C. *J. Chem. Phys.* **2013**, *139*, 084114−084114.
(19) Schirmer, J. *Phys. Rev. A* **1981**, *26*, 2395−2416.
(20) Starcke, J. H.; Wormit, M.; Dreuw, A. *J. Chem. Phys.* **2009**, *130*, 024104−024104.
(21) Schirmer, J.; Trofimov, A. B. *J. Chem. Phys.* **2004**, *120*, 11449−11449.
(22) Dutoi, A. D.; Cederbaum, L. S.; Wormit, M.; Starcke, J. H.; Dreuw, A. *J. Chem. Phys.* **2010**, *132*, 144302−144302.
(23) Trofimov, A. B.; Schirmer, J. *J. Phys. B* **1995**, *28*, 2299−2324.
(24) Langhoff, S. R.; E. R. Davidson, E. R. *Int. J. Quantum Chem.* **1974**, *8*, 61−72.
(25) Koch, H.; Jensen, H.; Jorgensen, P.; Helgaker, T. *J. Chem. Phys.* **1990**, *93*, 3345−3350.
(26) Liu, X.; Fatehi, S.; Shao, Y.; Veldkamp, B. S.; Subotnik, J. E. *J. Chem. Phys.* **2012**, *136*, 161101−161101.
(27) Helgaker, T.; Olsen, J.; Jorgensen, P. *Molecular Electronic-Structure Theory*; Wiley: New York, 2013; p 86.
(28) Laikov, D.; Matsika, S. *Chem. Phys. Lett.* **2007**, *448*, 132−137.
(29) Shao, Y. *Phys. Chem. Chem. Phys.* **2006**, *8*, 3172−3191.
(30) Because of its large size, we were unable to obtain the exact CISD energies for the PYCM molecule in section IV.A.1. However, we estimated the CISD energies for S_i, $i \in \{0, 1, 2\}$, in two different (and consistent) ways. First we ran exact CISD calculations with Q-Chem; the residuals of these calculations have not converged even after 30 iterations, even though the energies "appear converged" to within 0.01 eV. Second, with the GAMESS program, we ran three different CISD calculations, each with a different number of frozen (inactive) occupied orbitals: namely, 40, 35, and 30. These numbers can be fit quite well with a linear fit. Since the true number of core orbitals for the PYCM molecule is 14, we extrapolated our frozen core values to the case of 14 core orbitals. Both approaches above gave very similar

results (differing by less than 0.6 eV). In Figure 1, we plot the (as of yet not fully converged) Q-Chem data.
(31) Bixon, M.; Jortner, J.; Verhoeven, J. W. *J. Am. Chem. Soc.* **1994**, *16*, 7349−7355.
(32) Pasman, P.; Rob, F.; Verhoeven, J. W. *J. Am. Chem. Soc.* **1982**, *104*, 5127−5133.
(33) Krylov, A. I. *Annu. Rev. Phys. Chem.* **2008**, *59*, 433−462.
(34) Becke, A. D. *J. Chem. Phys.* **1993**, *98*, 1372−1377.
(35) Chai, J. D.; Head-Gordon, M. *J. Chem. Phys.* **2008**, *128*, 084106−084106.
(36) Dreuw, A.; Weisman, J. L.; Head-Gordon, M. *J. Chem. Phys.* **2003**, *119*, 2943−2946.
(37) Dreuw, A.; Head-Gordon, M. *J. Am. Chem. Soc.* **2004**, *126*, 4007−4016.
(38) Magyar, R. J.; Tretiak, S. *J. Chem. Theory Comp.* **2007**, *3*, 976−987.
(39) Neugebauer, J.; Louwerse, M. J.; Baerends, E. J.; Wesolowski, T. A. *J. Chem. Phys.* **2005**, *122*, 094115−094115.
(40) Lange, A. W.; Herbert, J. M. *J. Chem. Theory Comp.* **2007**, *3*, 1680−1690.
(41) Bernasconi, L.; Sprik, M.; Hutter, J. *J. Chem. Phys.* **2003**, *119*, 12417−12431.
(42) Savin, A. In *Recent Advances in Density Funtional Methods*; Chong, D. P., Ed.; World Scientific, 1995; pp 129−154.
(43) Savin, A.; Flad, H. J. *Int. J. Quantum Chem.* **1995**, *56*, 327−332.
(44) Gill, P. M. W.; Adamson, R. D.; Pople, J. A. *Mol. Phys.* **1996**, *88*, 1005−1009.
(45) Tawada, Y.; Tsuneda, T.; Yanagisawa, S.; Yanai, T.; Hirao, K. *J. Chem. Phys.* **2004**, *120*, 8425−8433.
(46) Song, J. W.; Hirosawa, T.; Tsuneda, T.; Hirao, K. *J. Chem. Phys.* **2007**, *126*, 154105−154105.
(47) Yanai, T.; Tew, D. P.; Handy, N. C. *Chem. Phys. Lett.* **2004**, *393*, 51−57.
(48) Vydrov, O. A.; Heyd, J.; Krukau, A. V.; Scuseria, G. E. *J. Chem. Phys.* **2006**, *125*, 234109−234109.
(49) Henderson, T. M.; Janesko, B. G.; Scuseria, G. E. *J. Chem. Phys.* **2008**, *128*, 194105−194105.
(50) Rohrdanz, M. A.; Herbert, J. M. *J. Chem. Phys.* **2008**, *129*, 034107−034107.
(51) Rohrdanz, M. A.; Martins, K. M.; Herbert, J. M. *J. Chem. Phys.* **2009**, *130*, 054112−054112.
(52) Lange, A. W.; Rohrdanz, M. A.; Herbert, J. M. *J. Phys. Chem. B* **2008**, *112*, 6304−6308.
(53) Baer, R.; Livshits, E.; Salzner, U. *Annu. Rev. Phys. Chem.* **2010**, *61*, 85−109.
(54) Levine, B. G.; Chaehyuk Ko, J. Q.; Martinez, T. J. *Mol. Phys.* **2006**, *104*, 1039−1051.
(55) Nitzan, A. *Chemical Dynamics in Condensed Phases*; Oxford University Press: USA, 2006; p 429.
(56) Schreiber, M.; Silva-Junior, M. R.; Sauer, S. P.; Thiel, W. *J. Chem. Phys.* **2008**, *128*, 134110−134110.
(57) Martinez, T. J.; Ben-Nun, M.; Levine, R. D. *J. Phys. Chem.* **1996**, *100*, 7884−7895.
(58) Ben-Nun, M.; Martinez, T. J. *J. Chem. Phys.* **2000**, *112*, 6113−6121.
(59) Barbatti, M.; Paier, J.; Lischka, H. *J. Chem. Phys.* **2004**, *121*, 11614−11624.
(60) Mori, T.; Glover, W. J.; Schuurman, M. S.; Martinez, T. J. *J. Phys. Chem. A* **2012**, *116*, 2808−2818.
(61) Crespo, R.; Teramae, H.; Antic, D.; Michl, J. *Chem. Phys.* **1999**, *244*, 203−214.
(62) Saebo, S.; Pulay, P. *Annu. Rev. Phys. Chem.* **1993**, *44*, 213−236.
(63) Gordon, M. S.; Schmidt, M. W. In *Theory and Applications of Computational Chemistry: The First Forty Years*; Dykstra, C. E., Frenking, G., Kim, K. S., Scuseria, G. E., Eds.; Elsevier: Amsterdam, 2005; p 1167.
(64) Mead, C. A.; Truhlar, D. G. *J. Chem. Phys.* **1982**, *77*, 6090−6098.
(65) Newton, M. D. *Chem. Rev.* **1991**, *91*, 767−792.
(66) Baer, M. *Chem. Phys. Lett.* **1975**, *35*, 112−118.
(67) Voorhis, T. V.; Kowalczyk, T.; Kaduk, B.; Wang, L. P.; Cheng, C. L.; Wu, Q. *Annu. Rev. Phys. Chem.* **2010**, *61*, 149−170.
(68) Cave, R. J.; Newton, M. D. *Chem. Phys. Lett.* **1996**, *249*, 15−19.
(69) Voityuk, A. A.; Rosch, N. *J. Chem. Phys.* **2002**, *117*, 5607−5616.
(70) Hsu, C. P.; You, Z. Q.; Chen, H. C. *J. Phys. Chem. C* **2008**, *112*, 1204−1212.
(71) Chen, H. C.; You, Z. Q.; Hsu, C. P. *J. Chem. Phys.* **2008**, *129*, 084708−084708.
(72) Hsu, C. P. *Acc. Chem. Res.* **2009**, *42*, 509−518.
(73) Wu, Q.; VanVoorhis, T. *J. Chem. Theory Comp.* **2006**, *2*, 765−774.
(74) Subotnik, J. E.; Cave, R. J.; Steele, R. P.; Shenvi, N. *J. Chem. Phys.* **2009**, *130*, 234102−234102.
(75) Fatehi, S.; Alguire, E.; Subotnik, J. E. *J. Chem. Phys.* **2013**, *139*, 124112.
(76) Alguire, E. C.; Fatehi, S.; Shao, Y.; Subotnik, J. E. *J. Phys. Chem. A* **2014**, DOI: 10.1021/jp411107k.
(77) Edmiston, C.; Ruedenberg, K. *Rev. Mod. Phys.* **1963**, *35*, 457−464.
(78) Foster, J. M.; Boys, S. F. *Rev. Mod. Phys.* **1960**, *32*, 300−302.
(79) F.Boys, S. In *Quantum Theory of Atoms, Molecules and the Solid State*; Lowdin, P., Ed.; Academic Press: New York, 1966; p 253.
(80) Werner, H.-J.; Knowles, P. J. *J. Chem. Phys.* **1988**, *89*, 5803−5814.
(81) Neese, F. *J. Chem. Phys.* **2003**, *119*, 9428−9443.